A Low Turbulence Recirculating Wind Tunnel for MEMS Sensor Characterization

Submitted By
Yucheng Sha

IN PARTIAL FULFILLMENT OF THE REQUIREMENTS FOR THE DEGREE OF

MASTER OF SCIENCE IN MECHANICAL ENGINEERING

School of Engineering
Tufts University
Medford, Massachusetts

May 2020

Signature of Author:
Yucheng Sha

Certified By:
Dr. Robert D. White
Department of Mechanical Engineering
Tufts University

Committee:
Dr. Chris Rogers
Department of Mechanical Engineering
Tufts University

Committee:
Dr. Jonathan P. Merrison
Department of Physics and Astronomy
Aarhus University, Denmark

Abstract

A laboratory scale low turbulence recirculating wind tunnel capable of Mach 0.5 operation has been designed and partially manufactured. A full tunnel model is used to calculate a pressure drop through the full circuit of almost 5000 Pa (at Ma 0.5). The major pressure drops are through the wide angle diffuser, test section, and shallow angle diffuser, which account for 1400 Pa, 1000 Pa, and 2500 Pa of pressure drop, respectively. The test section size of 50 mm (2 inches) by 100 mm (4 inches) is selected to allow Mach 0.5 to be achievable with flow volumes that can be provided by an affordable and reasonably sized blower. Based on the pressure drop and volume flow calculations, a blower, NYB Size 2110A20 Pressure Blower Arr. 4 CW-UB, is selected with a fan speed of 3500 rpm at maximum flow.

The thesis details design, design calculations, and fabrication of the test section, contraction, settling chamber, diffuser and wide angle diffuser. In addition to the primary pressure drop calculations, loading calculations and tests were conducted to ensure safe operation without mechanical failure over the expected pressure loads. The specific methods used to manufacture each component are detailed.

Plans for future measurements have also been described. Pitot-static tubes and pressure taps will characterize the flow speed and static pressure. Turbulent intensity will be measured by using a hot-wire anemometer. The primary application of the Tufts tunnel will be characterization of surface flows using low profile MEMS sensors. This extends previous work by the group at Tufts on MEMS microphone arrays and surface shear sensors for boundary layer measurement. The wall of test section in the Tufts tunnel will be modified by mounting several mesh elements, glass beads, fences, steps, and boundary

layer elements to produce different flow scenarios for extensive testing of MEMS aerodynamic sensor technologies. These methods will allow us to achieve a variety of time-averaged velocity and boundary layer profiles and unsteady flow features.

Acknowledgements

I would like to thank my advisor, Professor Robert White, who has, since I decided to finish a thesis to get my degree of master's at Tufts University, advised and supported my academic career as a graduate student. I was affected a lot from his advisor on my technical skills, academic knowledge and communication skills, and I could not gain so many experiences and skills without his guidance. I would also like to thank my second advisor, Professor Chris Rogers, who has given me several suggestions in my direction of my academic experience: wind tunnel program. I would like to thank my third advisor Professor Jonathan Merrison from Aarhus University, Denmark as well, who has done a lot in reviewing my thesis and giving feedback.

I am grateful for the generous technical support and advise from Bray Lab and Nolop Lab staff in Tufts University. I would like to thank Benjamin Ginden who has helped me a lot throughout my process to build the Tufts Wind Tunnel. He gave me advice on manufacturing and trained me to operate devices at Bray Lab. I learned many building skills during this experience. I would also like to thank James Aronson who has also helped me to operate devices and tools in Bray Lab. In addition, I would like to thank Brandon Stafford, who has provided a lot of guidance in manufacturing for me and helped me to use large devices like table saw and drill press. He supported me throughout my process of building each part through the whole wind tunnel. I am also grateful the support of the Department of Mechanical Engineering at Tufts for offering such an opportunity that I could improve myself as a graduate student.

Finally, I'd like to thank all my graduate school friends both for technical supports and for afterschool activities. I wish they could also have a good academic career. I

would like to thank my family who has always stand by me and gave me guidance during my lifetime. I am forever grateful for all the love and support from people who has been a part of this experience.

Table of Contents

Table of Figures

Table of Tables

1 Introduction

1.1 *Introduction*

Wind tunnels are a critical laboratory tool for the investigation of novel aero systems, for the validation of computational methods and models, and for the validation and exploration of new aerodynamic measurement technologies. They are used to imitate the actions of an object in flight to find out how the vehicles move [1]. Some of them can hold full-size versions of vehicles like aircrafts, cars and other ground vehicles. While some of them are just small one and can only hold small vehicles models or even sensors (if the test section is small enough and cannot put any model items in it). The wind tunnel moves air around an object or a sensor, making it seem like the object is really moving or flying [1]. Nowadays, wind tunnels are divided into three kinds of use: for government, for industry and for university. We will focus on a wind tunnel for university and want to design and build a special wind tunnel for our lab for MEMS sensor characterization.

Our goal is to build a wind tunnel to achieve sufficient turbulent energy in the boundary layer for aeroacoustics experiments and high wall shear for surface shear sensor experiments with high speed (0.5 Mach). We want to see if we can design a small wind tunnel with high velocity but its free stream turbulence is low enough in the test section. In addition, we want to build a small-size and low-cost wind tunnel to fit our lab, because it will be put microphone array and MEMS sensors (which are finished in past Tufts research) instead of real objects like vehicle models. It is a suitable opportunity to check the quality of our wind tunnel between calculation results and experimental results, and we can check

our microphone array and MEMS sensors whether they are able to work well on our wind tunnel.

1.2 *Contribution*

This wind tunnel model, depicted in figure 1-1, is a subsonic closed-circuit wind tunnel. We will follow this design to build the whole tunnel. Ethan Laverack and Kevin Holbrook have already built the contraction with fiber glass, and the 2 inch by 4 inch testing section with acrylic in Fall of 2016. My contribution is designing and building of the diffuser, wide angle diffuser, settling chamber and combining them together. To determine the choice of blower and which materials and structures we selected, I calculated the pressure drop of each part through the wind tunnel. In addition, I made a list for future measurements using the tunnel we built. All these things will be detailed in the following chapters.

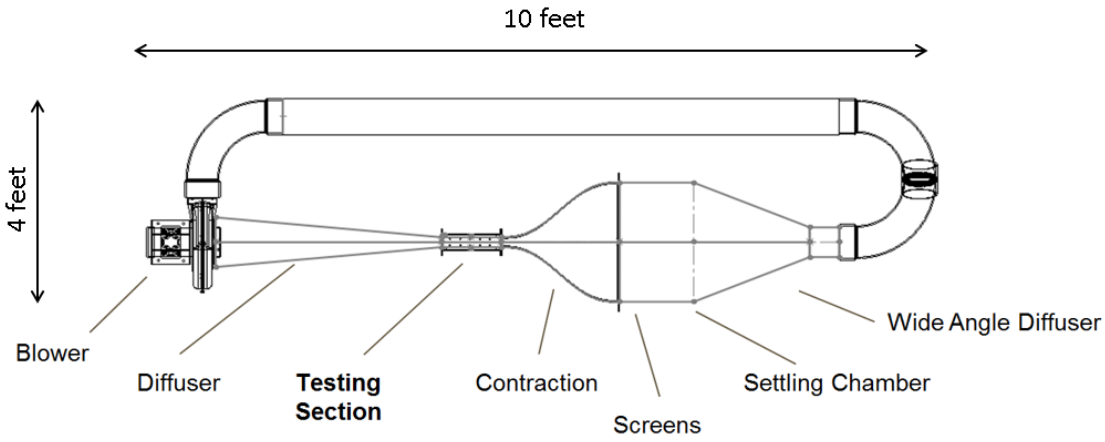

Figure 1-1 Tufts Wind Tunnel Model

In this thesis, chapter 2 will focus on the background of the wind tunnel, including the types, parts and several universities' models of wind tunnels. Chapter 3 is details of my calculation of pressure drop in each part. In chapter 4, we show how we design and build

each part of the wind tunnel. Chapter 5 contains the plans for future measurements using our wind tunnel.

2 Background

2.1 *Types of Wind Tunnel*

There are two types of wind tunnel classified by path of the air: open return wind tunnel and closed return wind tunnel. Firstly, in figure 2-1, we show a schematic drawing of "open return" wind tunnel, or open-circuit wind tunnel. This type of tunnel is also called an Eiffel tunnel, after the French engineer, or an "NPL tunnel", after the National Physical Laboratory in England, where the tunnel was first used [1]. This kind of tunnel has an open test section. In the tunnel, the air that passes through the test section is gathered from the surroundings in which the tunnel is located. The arrows on the figure denote the flow of air through the wind tunnel and around the room.

The open return tunnel has some advantages and some disadvantages. Open return wind tunnels require low construction costs and have advantages for propulsion and smoke visualization, and there is no accumulation of exhaust products. However, this type of tunnel has high operating costs because the fan must continually accelerate flow through the tunnel and can causes substantial noise. In addition, in the testing section, the flow quality will be poor and requires extensive screens and flow straighteners, due to the effects of the flow turning the corner into the bell mouth. It should be kept away from objects indoor and can be influenced by atmosphere and weather as well [1].

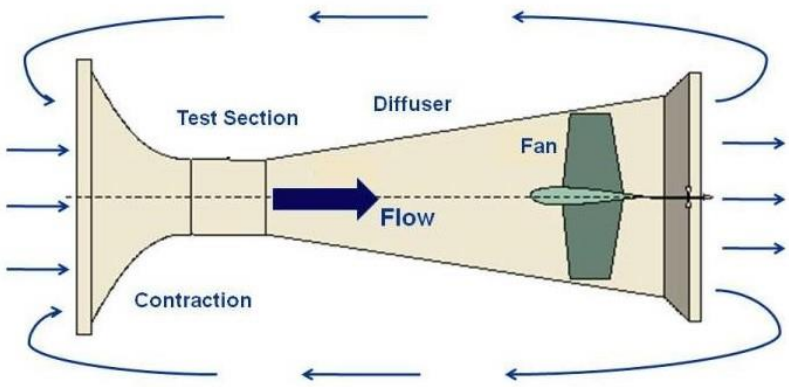

Figure 2-1 Open Return Wind Tunnel
taken from NASA: https://www.grc.nasa.gov/www/k-12/airplane/tunoret.html

Secondly, in figure 2-2, we show a schematic drawing of a "closed return" wind tunnel, or closed-circuit wind tunnel. This type of tunnel is also called a Prandtl tunnel, after the German engineer, or a "Gottingen tunnel" , after the research laboratory in Germany where the tunnel was first used [1]. In the closed return tunnel, air is routed from the exit of the test section back to the fan by a series of turning vanes. Exiting the fan, the air is returned to the contraction section and back through the test section. Air is continuously circulated through the duct work of the closed return tunnel and so it neither draws nor returns air to the surroundings. The arrows on the figure denote the flow of air through the wind tunnel.

The closed return tunnel has some advantages and some disadvantages. Closed return wind tunnels have improved flow quality in the test section because of the flow turning vanes in the corner and flow straighteners near the test section. It also requires low operating costs and less noise. However, this type of tunnel requires more construction costs with the added vanes and ducting. In addition, the tunnel must purge exhaust products accumulating in the tunnel, and so can be a poor design for propulsion and smoke visualization. It also may be necessary to employ heat exchanges or active cooling to avoid heating of the recirculating air.

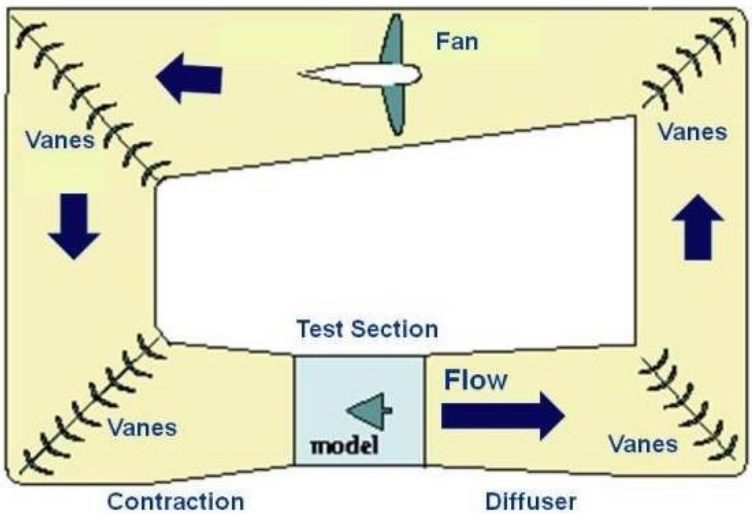

Figure 2-2 Closed Return Wind Tunnel
taken from NASA: https://www.grc.nasa.gov/www/k-12/airplane/tuncret.html

Another classification is based the maximum speed of the flow through the wind tunnel. It is typical to use the ratio of the speed of the fluid to the speed of sound. That ratio is called the Mach number (Ma), named after Ernst Mach, the 19th century physicist. The classification is summarized in Table 2-1.

$$Ma = u/a \quad (1)$$

u is the speed of flow while a is the speed of sound [1].

Table 2-1 Name of flow vs. Flow speed

Range of the Mach number , Ma	Name of flow , or conditions
Ma<1	Subsonic
Ma=1, or near 1	Transonic
1<Ma<3	Supersonic
3<Ma<5	High supersonic
Ma>5	Hypersonic
Ma>>5	High hypersonic

In next section, we will show some models in the university all around the world to see why they design and build the wind tunnels as they are.

2.2 *Universities' Wind Tunnel Models*

In this section, we will show some different models of university wind tunnel all around the world. I want to find relationships between wind tunnels' size and flow speed in them and find how to design our wind tunnel. We select four typical wind tunnel examples showing some details and other wind tunnel models simply shown in table 2.

Tohoku University in Japan has a small low-turbulence wind tunnel whose structure is shown in figure 2-3. It is a closed-return wind tunnel and its size of test section is 0.508 m by 0.293 m. The flow velocity in test section is 5-70 m/s so it is a subsonic wind tunnel.

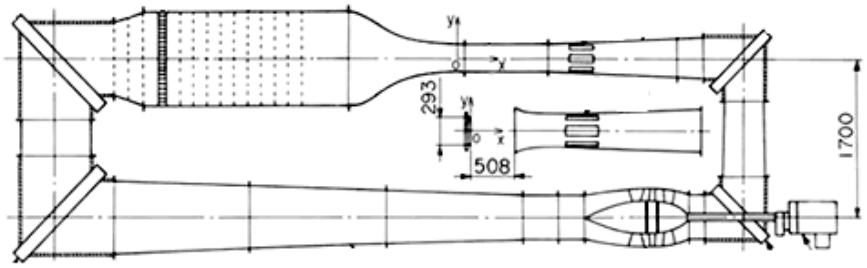

Figure 2-3 Wind Tunnel in Tohoku University
taken from Institute of Fluid Science, Tohoku University:

http://www.ifs.tohoku.ac.jp/windtunnel/english/setubi/kentei.html

University of Saskatchewan in Canada has a low speed wind tunnel whose structure is shown in figure 2-4. It is a subsonic closed-recircuit wind tunnel as well and its size of test section is 0.91 m by 1.13 m while its flow velocity in test section is 10-50 m/s. Many measurement instrumentations can be employed to this tunnel, like six-component force balances, pressure transducers, seven-hole pressure probe, hot-wire anemometry, laser Doppler velocimetry (LDV), and particle image velocimetry (PIV).

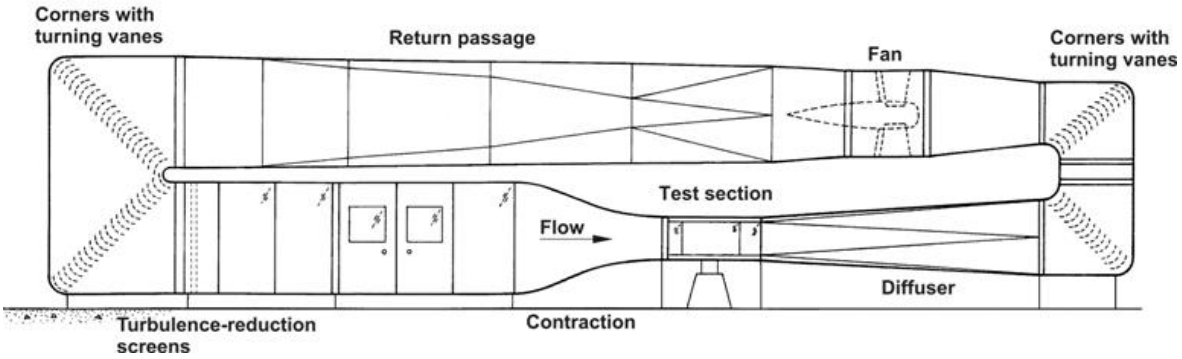

Figure 2-4 Wind Tunnel in University of Saskatchewan
taken from Department of Mechanical Engineering, University of Saskatchewan:

http://homepage.usask.ca/~drs694/research%20facilities.htm

Glenn L. Martin wind tunnel is a famous tunnel built in University of Maryland in America since 1949. Its structure and details are shown as figure 2-5 and 2-6. This wind tunnel is applied to perform tests for a wide range of vehicles like vertical takeoff aircraft, unmanned air vehicles and ground vehicles, therefore, it must be large enough. Its size of test section is 7.75 foot by 11.04 foot and the flow velocity is Mach 3. This wind tunnel is a supersonic closed return wind tunnel.

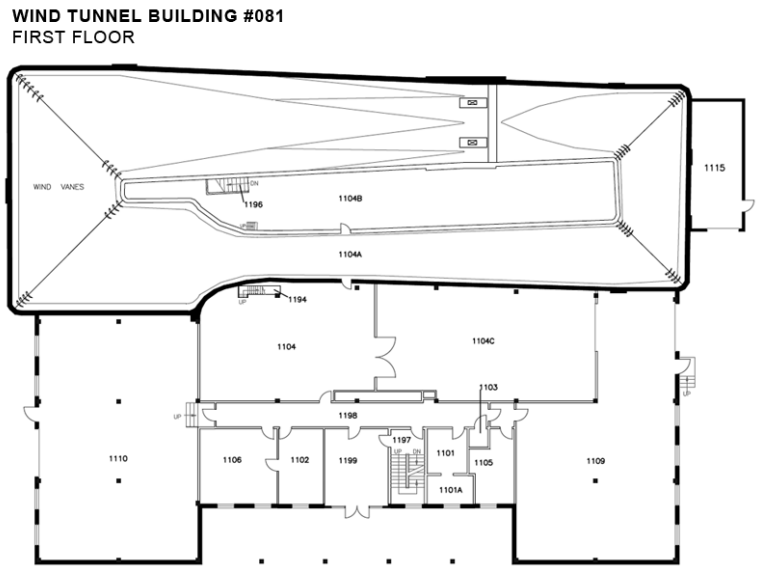

Figure 2-5 Wind Tunnel in University of Maryland
taken from A. James Clark School of Engineering, University of Maryland:
https://windtunnel.umd.edu/about-us

Figure 2-6 Glenn L. Martin Wind Tunnel
taken from A. James Clark School of Engineering, University of Maryland:

https://windtunnel.umd.edu/about-us

Other university wind tunnel examples are shown below:

Table 2-2 Other Universities' Wind Tunnel examples (2, 15-20)

Name	University	Location	Flow Speed	Testing Section Size
Low speed wind tunnel	Purdue University	America	100 ft/sec Subsonic	12" by 18"
Closed-loop Subsonic wind tunnel	University of Leeds	British	2-15 m/s Subsonic	0.5 m by 0.5 m
Variable Mach number supersonic wind tunnel	University of Michigan	America	Mach 1.3-4.6 Supersonic	4" by 4"
HyperTERP	University of Maryland	America	Mach 6 Hypersonic	300 mm by 300 mm

In next section we will turn to describe the details of each part through an entire wind tunnel about where the location they are put and what they are used for.

2.3 *Parts of Wind Tunnel*

In this section, the main parts of the wind tunnel will be described. Figure 2-7 shows again the main parts of our Tufts wind tunnel design.

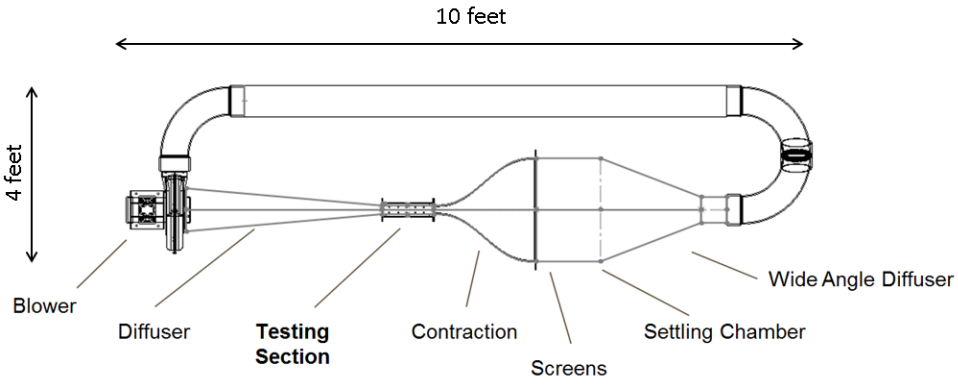

Figure 2-7 Closed Return Wind Tunnel Model

A whole closed-circuit wind tunnel is combined by several parts: Testing Section, Contraction, Diffuser, Wide Angle Diffuser, Settling Chamber with screens and honeycomb, Corners, Return Ducts and Blowers.

2.3.1 Test Section

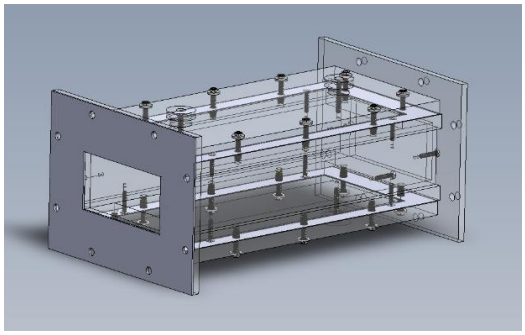

Figure 2-8 Design of Tufts Test Section

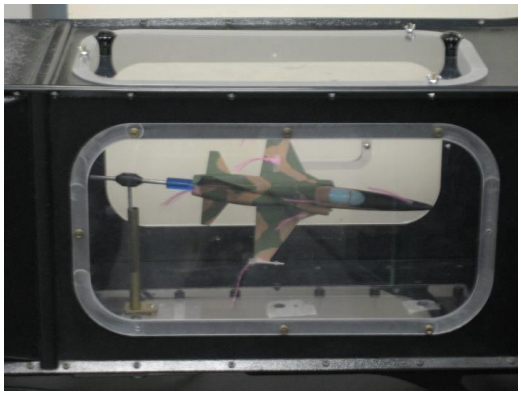

Figure 2-9 example from NASA Tunnel's Test Section
taken from NASA: https://www.grc.nasa.gov/www/k-12/airplane/tunpart.html

Test section, shown as Figure 2-8 and 2-9 is the part to do experiments where the models or shear sensors are placed. It has the smallest size, but flow move fastest and with lowest turbulence through the whole tunnel [3, 8-10,29-30].

2.3.2 Contraction

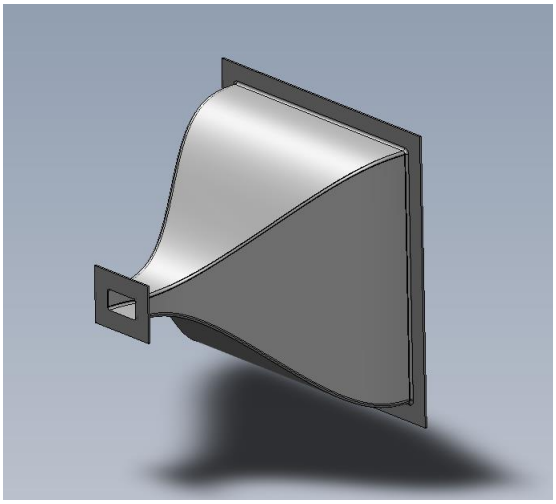

Figure 2-10 Contraction

Contraction follows the settling chamber and is used to accelerate the flow velocity to meet the requirements of testing section which is just the next part. The conservation of mass smoothly moves through this part from a low velocity to a very high velocity by its ratio of size between its entrance and exit. It is very important to keep the flow goes

smoothly so the curves along the part are very useful to keep the air uniform, steady and stable [3-4, 7-10, 29-30]. Our shape of contraction will be shown in chapter 4 about building of wind tunnel.

2.3.3 Diffuser

Diffuser is between the testing section and blower, which is usually the high-loss segment, and can critically affect the flow through the whole wind tunnel. Diffuser widens the area of cross-section area so that the flow will decelerate to prevent the turbulence. And it also used to transfer the kinetic energy to pressure energy to reduce the energy loss through the tunnel.

When we design this part, we should prevent the flow separation which can cause pressure fluctuations and turbulence through testing section. To achieve this goal, the angle of the diffuser should not exceed 6 degrees (when losses caused by friction and by pressure expansion are the same, the whole loss of diffuser is the least) and diffuser area ratio should not exceed 2.5 [5-9].

2.3.4 Wide Angle Diffuser

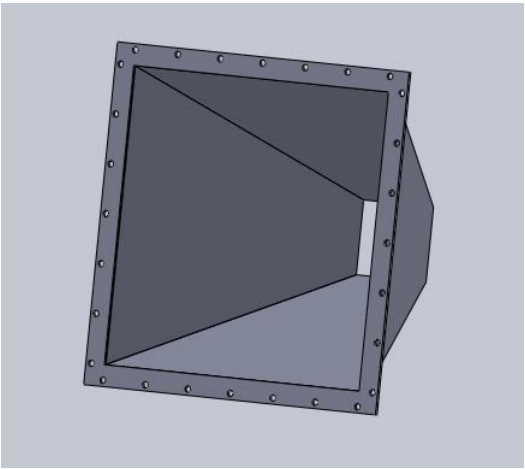

Figure 2-11 Wide Angle Diffuser

Wide angle diffuser is the part between the corner and settling chamber. It is to achieve lower flow velocity by rapidly increasing the area of cross-section in a very short length. Usually, the diffuser angle is up to 45 degrees[3,8]. Substantial turbulence may be generated at this stage, we can put a large screen in it to keep flow from separation, and also requiring the settling chamber, screens, honeycombs and contraction as described in other sections to remove turbulence energy and straighten the flow.

2.3.5 Settling Chamber

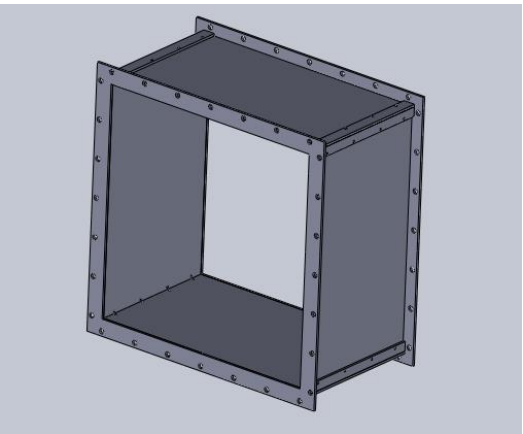

Figure 2-12 Settling Chamber

If the flow from settling chamber is not uniform and steady, the flow through contraction and test section will unsteady and unstable as well, which could cause flow separation and additional turbulence. Therefore, settling chamber is the place where we can put screens and honeycombs in it to keep the flow steady and stable in the following parts: contraction and test section. Settling chamber should designed with a suitable length to add enough screens and honeycombs [3-10, 29-30].

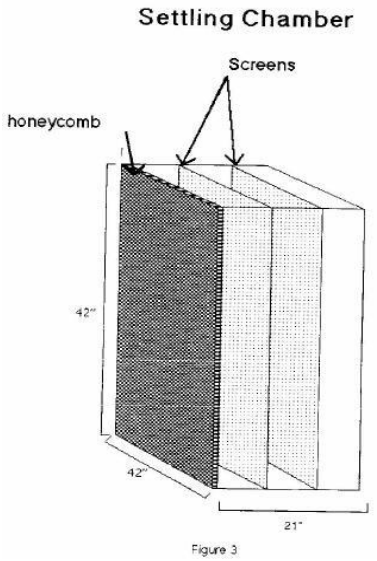

Figure 2-13 Screens & Honeycomb in settling chamber
taken from NASA: https://www.grc.nasa.gov/www/k-12/WindTunnel/wandering_windtunnel.html

Honeycomb is used to straighten the flow and cut the large vortices into small ones to decrease the turbulence. It can also improve the distribution of flow velocity by friction through the honeycombs. Open return wind tunnel must add honeycombs because the air goes into the tunnel from every direction which means it is very unsteady while closed return wind tunnel is not necessarily fixed ones. There are three types of honeycomb: circle cell, square cell and regular hexagonal cell. Among these three, hexagonal honeycombs incur the lowest pressure drops and the most effective to reduce the turbulence [3-11].

Screens are used to reduce the turbulence through the settling chamber by cutting the large vortices into small ones like honeycombs. They are more effective to reduce axial turbulence than horizontal turbulence. Screens are always fixed behind the honeycomb because they don't have the function to straightening the flow. The denser and more layers of screens, the better affect to decrease flow fluctuations and turbulence, but the more energy loss of flow [3,8,9-11,32-33].

2.3.6 Corner

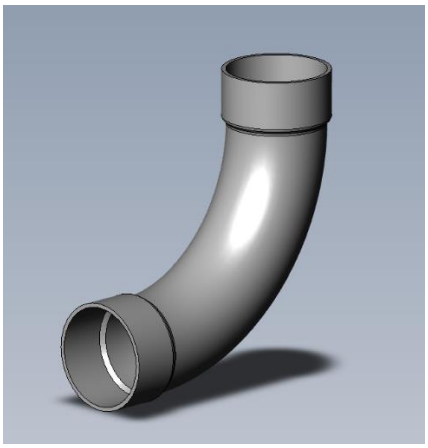

Figure 2-14 Corner

We usually need 4 corners to finish the 360-degree whole closed return process. The flow experiences the most pressure drop through the corners because it is easier to cause separation and vortices when flow moves through the corners. Therefore, we should add corner vanes to reduce the loss. Corner vanes can keep the centrifugal forces of flow working on themselves instead of the corner, which will prevent increasing pressure and make the flow move more smoothly as well [3,8-10, 29-30].

2.3.7 Blower

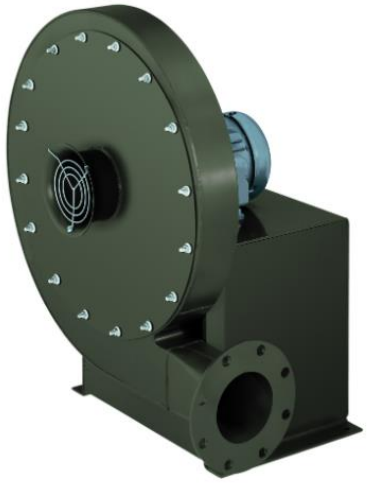

Figure 2-15 Blower
taken from New York Blower Company: https://www.nyb.com/pressure-blower/

Blower is a mechanical device to move the flow and determine the pressure of each part through the wind tunnel. We will use the following one: NYB Size 2110A20 Pressure Blower Arr. 4 CW-UB, which dimensions are the following:

Table 2-3 Blower Dimensions

Flow Velocity (cfm)	2000
Pressure (w.g.)	32.4
Horsepower (bhp)	14
Wheel Speed (rpm)	3500
Weight Net (lb/ft^3)	0.0695
Motor (HP)	20

The blower is sized to provide the required volume flow at the expected pressure drop based on the desired maximum flow speed at the test section and the pressure drop calculation as detailed in Chapter 3.

2.4 *Tufts MEMS Shear Sensor & Microphone Array*

2.4.1 MEMS (Microelectromechanical System) Shear Sensor

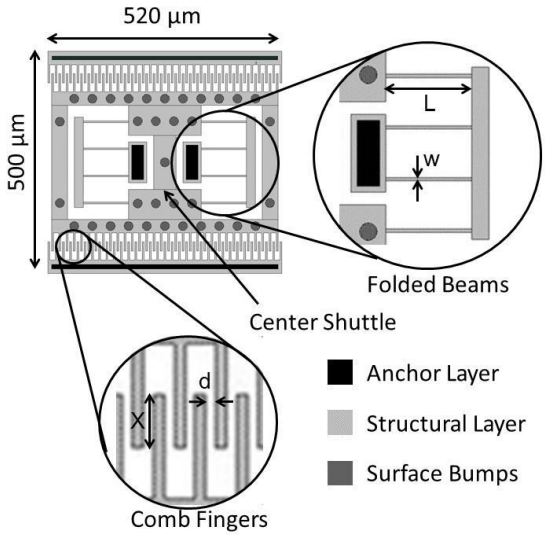

Figure 2-16 Diagram of the mechanical structure of the floating element sensor taken from Zhengxin Zhao's paper [13-14]

This kind of technology is called MEMS (Microelectromechanical system) fluid shear stress sensor from Tufts University, and it can also be called MEMS floating element sensor. We can use it to measure the shear stress of a flat plate boundary layer in a wind tunnel flow environment[14]. It can be applied to measure differential capacitance changing resulting from forces through the flow in a wind tunnel[13]. There are several advantages and disadvantages of the MEMS floating elements. This technology is easy to use and with high spatial and temporal resolution, and as the elements are directly respond to the wall, they are more accurately to measurement the shear stress. However, they are very sensitive to pressure gradients through the wall and possibly lack robustness and alignments during the crash between water and particles [13].

From Figure 2-16, it is the mechanical structure of the MEMS floating element sensor. There are four inner beams and outer fingers fixed on the substrate through the anchors. It is to decrease the influence of residual stresses during the manufacturing when the structure releasing. Below are the dimensions of the floating element sensor [14]:

Table 2-4 Dimensions of the floating element sensor

Finger gap, *d* (μm)	2.88
Finger width (μm)	5.13
Number of comb fingers per element, N	64
Thickness of structure, *t* (μm)	8.8
Width of folded beam, *w* (μm)	5.13
Length of folded beam, *L* (μm)	99.2
Height of bump (μm)	11.7
Diameter of bump (μm)	24.7
Air gap separation (μm)	5.2
Shuttle top area, *Am* (mm2)	0.096

2.4.2 Microphone Array

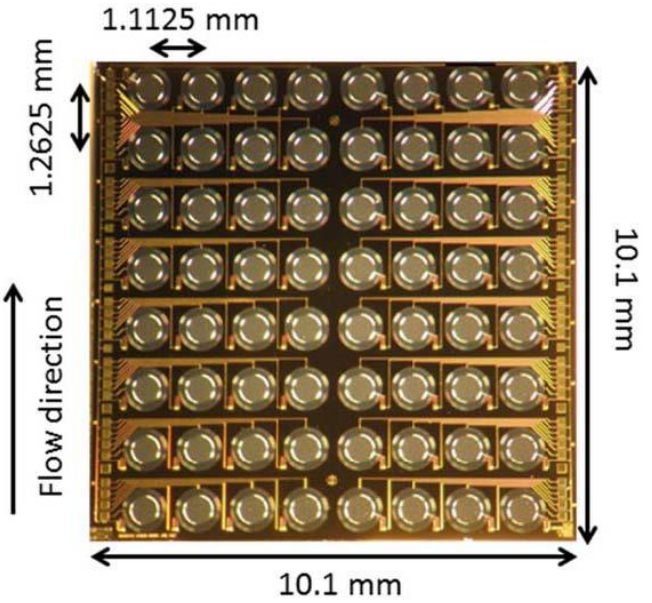

Figure 2-17 Photograph of the microphone array chip after microfabrication is complete but before the release etch or packaging process taken from Krause J S's paper [12]

Microphone array is a device by combining MEMS microphones together to measure the fluctuating pressure beneath a turbulent boundary layer (TBL), which is a kind of externally radiated noise in aircraft. We try to use it to reduce both internal and external noise caused by pressure fluctuations when designing the structure of the aircraft. From Figure 2-17, Each chip has 64 individual elements and measures 10.1 mm. This kind of microphone array can be applied to measure the single point turbulence spectra in a flow duct at Mach numbers up to 0.6 under a flat plate turbulent boundary layer [12].

3 Pressure Drop Calculation

In this Chapter, we will talk about the pressure drop through the whole Tufts wind tunnel design. Figure 3-1 shows again the parts of the wind tunnel we will calculate the pressure drop. We have calculated the pressure drop in each part below and will show calculation details in next section: test section, contraction, diffuser, wide angle diffuser, corners (there are 3 corners with the same size) and the return duct. We assumed flow through parts is incompressible (flow speed in each part except test section at 0.5 Ma is under 0.3 Ma, so we can assume it incompressible).

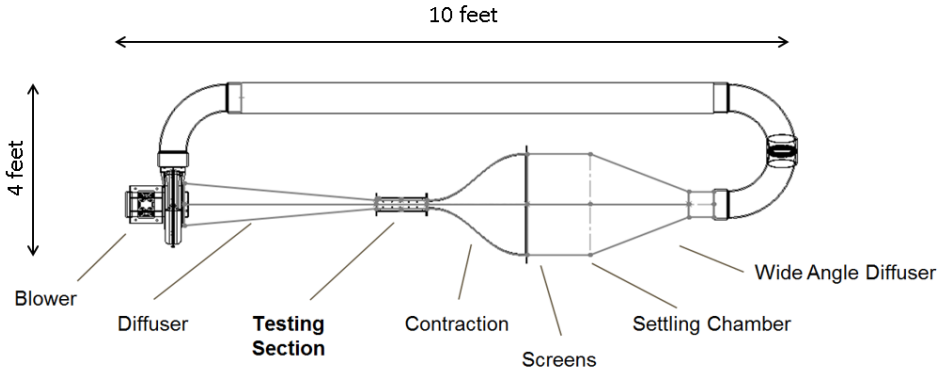

Figure 3-1 Wind Tunnel Model

We use the equation (1) to figure out the flow velocity in each part:

$$v = v_0(\frac{D_0}{D})^2 \qquad (1)$$

v and D are the flow velocity and hydraulic dimeter of the part you are calculating while v_0 and D_0 are the flow velocity and hydraulic dimeter of testing section. And there are several known constants:

Table 3-1 Some known constant

Constant	Means	Quantities
ρ	Density of flow	1.293 kg/m^3
μ	Viscosity Coefficient of flow	18.08e-6 kg/(m*s)
v_0	Center velocity in test section	0.1 Ma = 34 m/s
		0.3 Ma = 102 m/s
		0.5 Ma = 170 m/s

3.1 *Parts of Tufts Wind Tunnel*

3.1.1 Test Section

Our test section is a 12-inch long part, which means the L_0 is 0.3048 m and its hydraulic diameter D_0 is 8/3 in, equals 0.0678 m. The Reynolds number Re:

$$Re = \frac{\rho v_0 D_0}{\mu} \quad (2)$$

and friction coefficient λ (a dimensionless value to show friction of the surface) are different because of the velocity of flow moving in this part. I will show the Re and λ in the table 3-2 below:

Table 3-2 Reynolds number & friction coefficient vs. velocity of flow

	0.1 Ma	0.3 Ma	0.5 Ma
Re	0.165e6	0.495e6	0.824e6
λ	0.0128	0.0120	0.0116

Friction coefficient is from the figure 3-2 which is a graph related to Reynolds number.

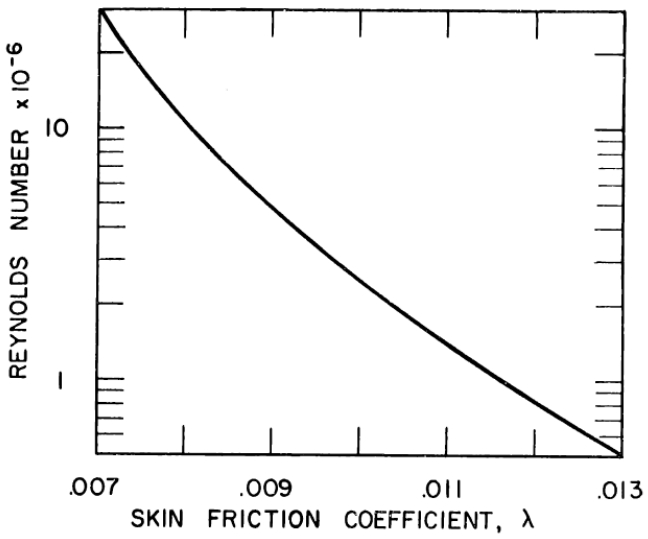

Figure 3-2 Friction coefficient vs. Re taken from Vlajinac's paper: [1]

The equation to calculate the pressure drop is below [7]:

$$\Delta p_1 = \lambda \frac{L_0}{D_0} \frac{1}{2} \rho v_0^2 \quad (3)$$

And the results of calculation are:

Table 3-3 Results of test section

	0.1 Ma	0.3 Ma	0.5 Ma
Δp_1 (Pa)	43	360	970

3.1.2 Contraction

The inlet diameter of contraction D_i is 24.25 inches which equals 0.61595 m. Its length L_{con} is 24 in equaling 0.6096 m. By using the equation (1), center velocity at inlet of contraction v_i is:

Table 3-4 Flow velocity at inlet of contraction

	0.1 Ma	0.3 Ma	0.5 Ma
v_i (m/s)	0.41	1.24	2.06

The equation to calculate the pressure drop is below [7]:

$$\Delta p_2 = \frac{\lambda}{4}\frac{L_0}{D_i - D_0}\left(1 - \left(\frac{D_0}{D_i}\right)^4\right)\frac{1}{2}\rho v_0^2 \qquad (4)$$

And the results of calculation are:

Table 3-5 Results of contraction

	0.1 Ma	0.3 Ma	0.5 Ma
Δp_2 (Pa)	1.33	11.22	30.12

3.1.3 Diffuser

The outlet diameter of the diffuser D_d is 10 inches which equals 0.254 m and the diffuser angle is 5 degrees. By using the equation (1), center velocity at outlet of diffuser v_d is:

Table 3-6 Flow velocity at outlet of diffuser

	0.1 Ma	0.3 Ma	0.5 Ma
v_d (m/s)	2.42	7.27	12.11

The equation to calculate the pressure drop is below [7]:

$$\Delta p_3 = \left[(3.14\lambda + 0.0262)\left(1 - \left(\frac{D_0}{D_d}\right)^4\right) + \left(\frac{D_0}{D_d}\right)^2\right]\frac{1}{2}\rho v_0^2 \qquad (5)$$

And the results of calculation are:

Table 3-7 Results of diffuser

	0.1 Ma	0.3 Ma	0.5 Ma
Δp_3 (Pa)	102	906	2500

3.1.4 Wide Angle Diffuser

The hydraulic diameter of wide angle diffuser D_{wad} is 0.61595 m while its diffuser angle is 21 degrees. By using the equation (1), center velocity at outlet of wide angle diffuser v_{wad} is:

Table 3-8 Flow velocity at outlet of wide angle diffuser

	0.1 Ma	0.3 Ma	0.5 Ma
v_{wad} (m/s)	0.41	1.24	2.06

The equation to calculate the pressure drop is below [7]:

$$\Delta p_4 = \left[(3.14\lambda + 0.0262)\left(1 - \left(\frac{D_0}{D_{wad}}\right)^4\right) + \left(\frac{D_0}{D_{wad}}\right)^2\right]\frac{1}{2}\rho v_0^2 \qquad (6)$$

And the results of calculation are:

Table 3-9 Results of wide angle diffuser

	0.1 Ma	0.3 Ma	0.5 Ma
Δp_4 (Pa)	58	510	1400

3.1.5 Return Duct

Our return duct is a 112.63-inch long part, which means the length L_{rd} is 2.8608 m. And its diameter is 0.1826 m. By using the equation (1), center velocity of return duct v_{rd} is:

Table 3-10 Flow velocity of return duct

	0.1 Ma	0.3 Ma	0.5 Ma
v_{rd} (m/s)	4.69	14.07	23.45

The equation to calculate the pressure drop is below [7]:

$$\Delta p_5 = \lambda \frac{L_{rd}}{D_{rd}} \left(\frac{D_0}{D_{rd}}\right)^4 \frac{1}{2} \rho v_0^2 \quad (7)$$

And the results of calculation are:

Table 3-11 Results of return duct

	0.1 Ma	0.3 Ma	0.5 Ma
Δp_4 (Pa)	2.9	24.0	64.6

3.1.6 Corners

Diameter of one corner is 0.16884 m. Reynolds number Re_{cor}

$$Re_{cor} = \frac{\rho v_{cor} D_{cor}}{\mu} \quad (8)$$

and friction coefficient are shown below as they change with different flow velocity. And by using equation (1), we can also get the center velocity of each corner v_{cor} below:

Table 3-12 Reynolds number, friction coefficient and velocity of corner vs. flow velocity

	0.1 Ma	0.3 Ma	0.5 Ma
Re	0.066e6	0.197e6	0.331e6
λ	0.0130	0.0126	0.0122
v_{cor} (m/s)	5.48	16.45	27.41

Friction coefficient is from the figure 3-2 which is a graph related to Reynolds number as well.

The equation to calculate the pressure drop is below [8]:

$$\Delta p_6 = n\left(0.10 + \frac{4.55}{(\ln Re_{cor})^{2.58}}\right)\left(\frac{D_0}{D_{cor}}\right)^4 \frac{1}{2}\rho v_0^2 \quad (9)$$

And the results of calculation are:

Table 3-13 Results of corners

	0.1 Ma	0.3 Ma	0.5 Ma
Δp_6 (Pa)	0.17	1.46	4.03

3.1.7 Summary

Table 3-14 Summary of pressure drop calculation

Part	Pressure Drop (Pa)	Center Velocity (m/s)	Flow Velocity in Test
Test Section Δp_1	43	34	0.1 Ma
	360	102	0.3 Ma
	970	170	0.5 Ma
Contraction Δp_2	1.33	0.41	0.1 Ma
	11.22	1.24	0.3 Ma
	30.12	2.06	0.5 Ma
Diffuser Δp_3	102	2.42	0.1 Ma
	906	7.27	0.3 Ma
	2500	12.11	0.5 Ma
Wide Angle Diffuser Δp_4	58	0.412	0.1 Ma
	510	1.236	0.3 Ma
	1400	2.06	0.5 Ma
Return Duct Δp_5	2.9	4.69	0.1 Ma
	24.0	14.07	0.3 Ma
	64.6	23.45	0.5 Ma
Corners Δp_6	0.17	5.48	0.1 Ma
	1.46	16.45	0.3 Ma
	4.03	27.41	0.5 Ma
Total $\Delta p = \sum_1^6 \Delta p_i$	**207**		**0.1 Ma**
	1812		**0.3 Ma**
	4968		**0.5 Ma**

From table 3-14, we can see that since the flow velocity of testing section increases, the pressure drop will increase as well. And diffuser causes the largest loss through the whole tunnel.

After calculating the pressure drop of each part through the wind tunnel, we will begin to build them and assembly them together to take experiments and check the real thing with our design. It will be described in Chapter 4.

4 Building the Tufts Wind Tunnel

In this Chapter, I will describe how we built the wind tunnel in details and what materials we select and what methods to put them together. For all the parts through the tunnel, we will show the final model we really build, while we will talk about the failure examples of diffuser as well because we took the most time to build it and we want to show why we choose the final method to build it. We will show construction in next section: test section, contraction, settling chamber, diffuser, wide angle diffuser and assembly.

Figure 4-1 Wind Tunnel Building

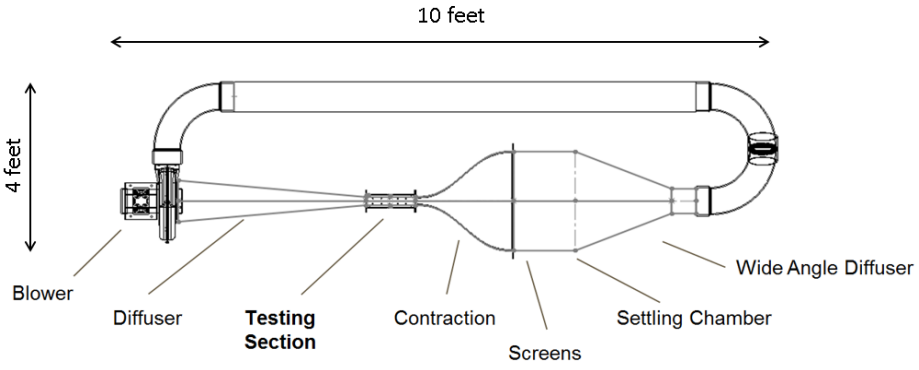

Figure 4-2 Tufts Wind Tunnel Design

Figure 4-1 is the structure of Tufts wind tunnel we already built, and it can be checked from our design of figure 4-2, which is shown repeatedly. For test section, settling chamber, diffuser and wide angle diffuser, we all built them from acrylic sheets while contraction is made from fiber glass.

4.1 *Parts of the wind tunnel*

4.1.1 Test Section

Our test section shown in Figure 4-3 is built from acrylic. Its cross-section size is 2 inch by 4 inch and its length is 1 foot. We want to reduce the turbulence through the test section so that the inner surface must be smooth. Since our test section is a small one, we can only test sensors in the wall, or wall roughness, instead of models like UAVs or ground vehicles models in the section. To be convenient, we designed the up and down surfaces detachable. When we want to put the sensors, or specialized structures on the inner surfaces, we can take off the up surface and put the sensors in.

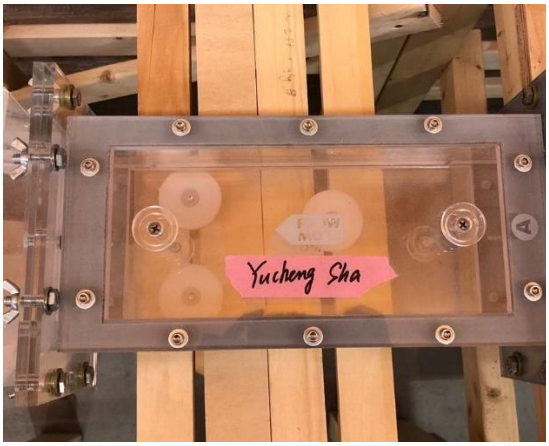

Figure 4-3 Test Section

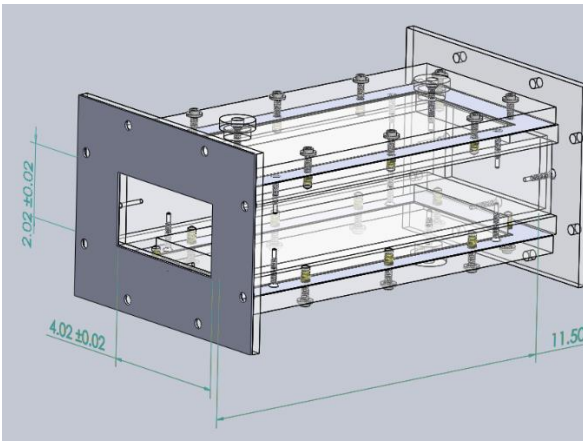

Figure 4-4 Design of Test Section

I will also show the details of the flanges on the test section in figure 4-5, which were made from 0.5-inch-thick acrylic sheets. Both the flanges and the up and down sides were

connected to the main part by screws. We firstly drilled holes just a bit smaller than the diameter of screws we used and glued them together.

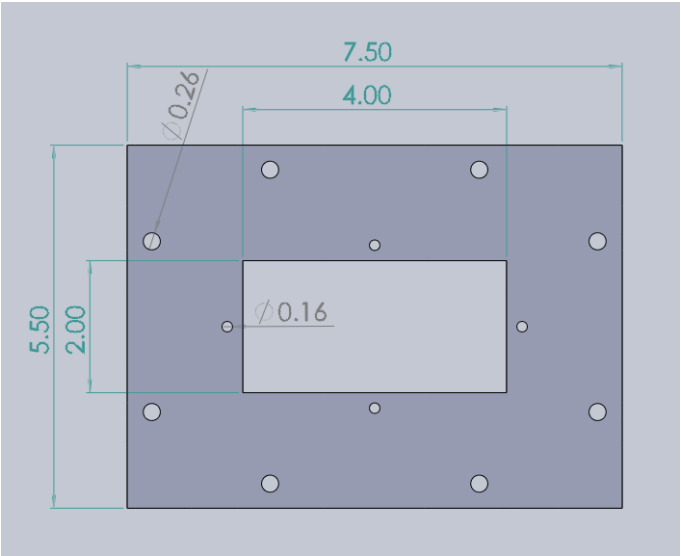

Figure 4-5 Flange Size of Test Section

4.1.2 Contraction

Contraction is made from fiber glass. The size is from 2 feet by 2 feet at inlet to 2 inch by 4 inch like test section at outlet and its length is 15 inches. The shape curve function is:

$$y = (\left(\frac{W}{2}\right) - \left(\frac{W}{2} - \frac{H}{2}\right)\left(\left(6\left(\frac{x}{L}\right)^5\right) - \left(15\left(\frac{x}{L}\right)^4\right) + (10\left(\frac{x}{L}\right)^3)\right))$$

Where W = 24 inches is the width of the inlet inches, H = 2 inches or 4 inches is the height of test section in two directions and L = 24 inches is the length of contraction. This function is a method called matched polynomial of 5 orders [29]. This curve is given in a sketching plane that is vertical cutting the contraction in two or horizontal, again in the center as shown in figure 4-8, and the curve are shown in figure 4-9 and 4-10. To reduce the turbulence and vorticities in the contraction and flowing to the test section, we made

sure that the inner surface is smooth. We also soldered the fiber glass as a whole construction to prevent leak and gaps. The flange of contraction outlet is the same size as the one of test section while the inlet flange will be detailed at settling chamber part next.

Figure 4-6 Contraction

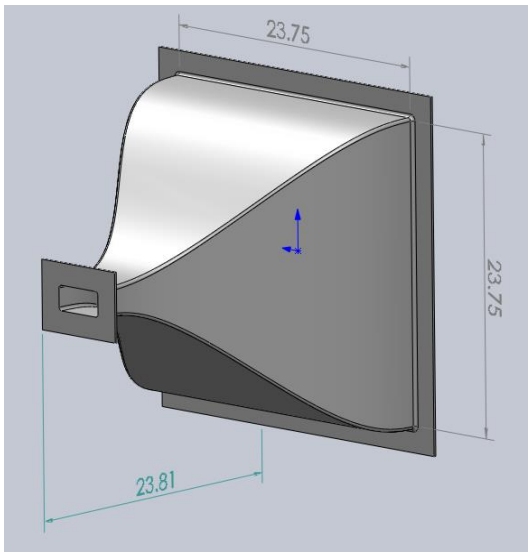

Figure 4-7 Design of Contraction

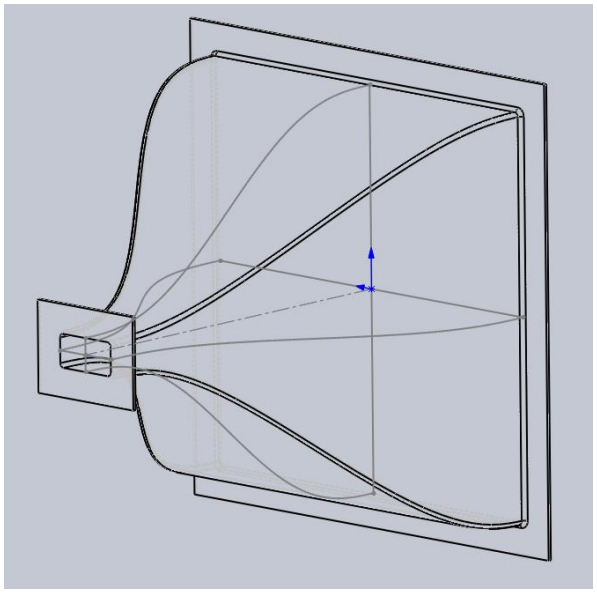

Figure 4-8 Sketching Plane in Contraction

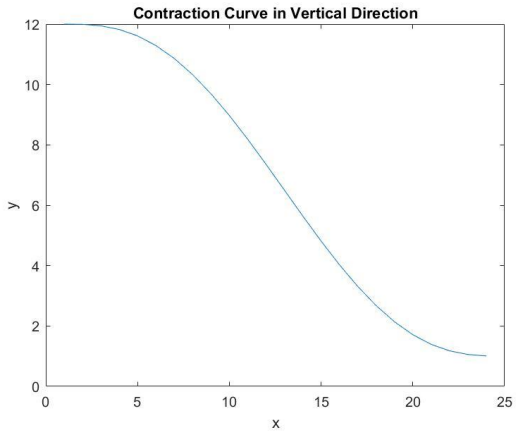

Figure 4-9 Contraction Curve 1

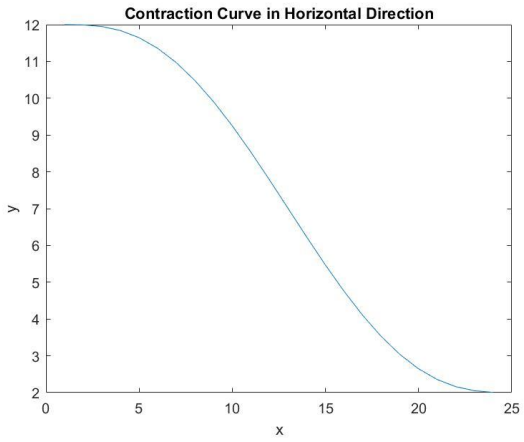

Figure 4-10 Contraction Curve 2

4.1.3 Settling Chamber

Our settling chamber rectangle with a cross section of 2 feet by 2 feet and its length is 14 inches. We built them from acrylic sheets with a thickness of 0.5 inch. There are 4 0.5 inch by 0.5 inch acrylic bars to connect 4 sides of settling chamber and it is also screwed by 0.25-inch-long heat-set inserts. The two flanges of inlet and outlet of settling chamber are the same size and they are the same as contraction inlet flange. The size is shown in figure 4-13.

Figure 4-11 Settling Chamber

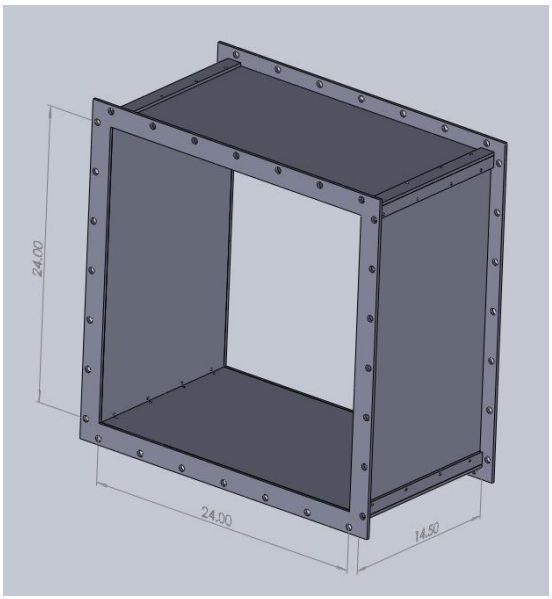

Figure 4-12 Design of Settling Chamber

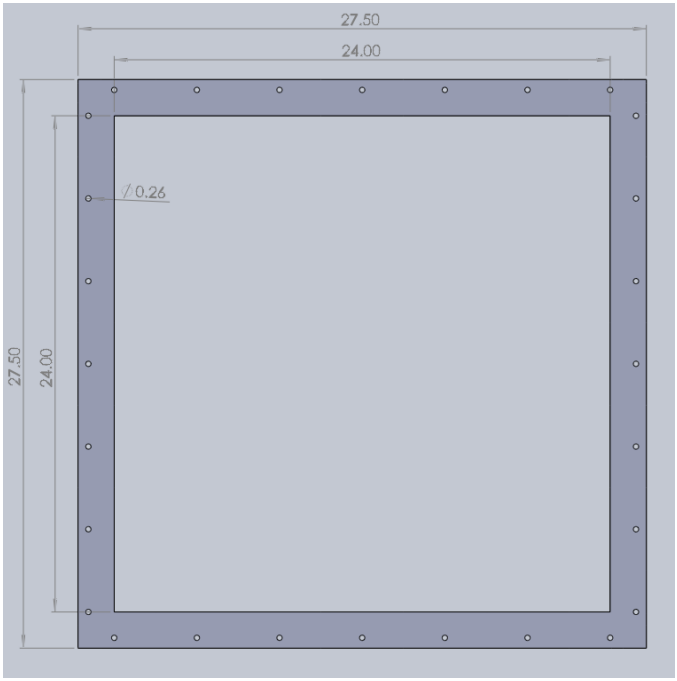

Figure 4-13 Flange of Settling Chamber

Figure 4-14 shows how we connected the two sides with the 0.5 inch by 0.5 inch acrylic bar. We selected 10-32 heat-set inserts as shown in figure 4-15 because the diameter of the inserts is 0.3048 inch which was suitable for the 0.5-inch-thick acrylic sides. After drilling

a smaller hole on the surface of one side, we put the heat-set inserts into the holes like figure 4-16 and screwed the sides and bars together to build the whole settling chamber. The inserts were used to build the diffuser and wide angle diffuser, which will be detailed in the following parts.

Figure 4-14 The Corner of Settling Chamber

Figure 4-15 Heat-set inserts

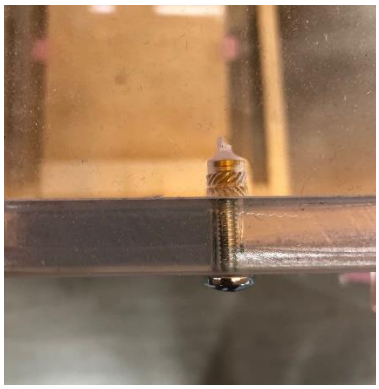

Figure 4-16 The Way to Put the Inserts

4.1.4 Diffuser

Our diffuser is divided into 2 parts because the whole section are 46 inches long while the acrylic sheets we used are just the size of 2 feet by 2 feet. Since the diffuser angle is 5 degrees, the diffuser extends from 2 inch by 4 inch like test section at inlet to a 10.2 inch by 10.2 inch square (a square is easier to design the following parts) at outlet. As shown in figure 4-17 and 4-18, we added 4 1 inch by 1 inch acrylic bars shown in figure 4-19 as the connection between 4 sides in both 2 parts, and add 4 joints shown in figure 4-20 and 4-21 (the size of these two kinds of joints are shown in figure 4-22 and 4-23) to connect two parts as well. The thickness of all the sides are 0.5 inch so to assembly all items together, we put 0.5-inch-long heat-set inserts on the outer surface of each side on bars and use screws which match the inserts. We designed the up and down sides larger than left and

right sides because we want to leave fewer gap between sides and sides and to make sure there are few leaks, we also glued every place where may cause leaks.

Figure 4-17 Diffuser 1

Figure 4-18 Diffuser 2

Figure 4-19 Acrylic Bars

Figure 4-20 Joint 1 to Connect Two Parts

Figure 4-21 Joint 2 to Connect Two Parts

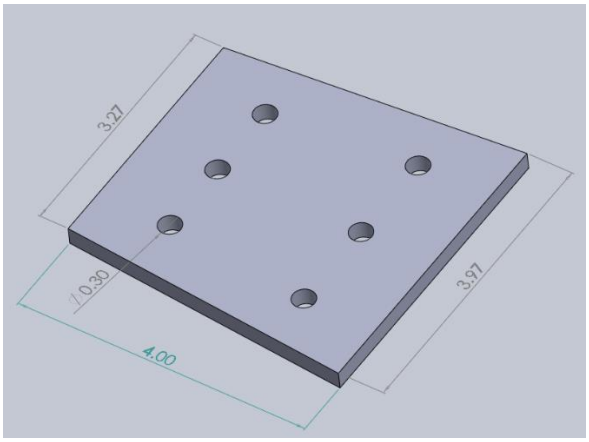

Figure 4-22 Joint 1 Size

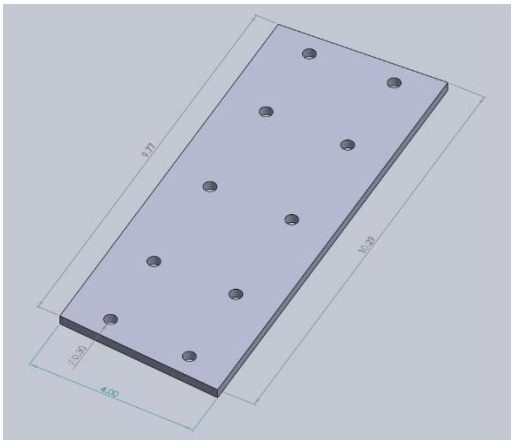

Figure 4-23 Joint 2 Size

It took the most time for us to build the diffuser because we tried several plans and finally chose the present one. Firstly, I wanted to design all the 4 sides with finger joints because we found from testing that finger joints could keep the connections more stable which is detailed in the section of 4.2. I built some small testing pieces but found it couldn't be possible to use, because when cutting these pieces in laser cutting, the frontiers of all the parts were always melted as our acrylic sheets are 0.5 inch thick, so it required very high temperature laser to cut them which could cause melting. Then the pieces were always smaller than what we wanted and caused many gaps between joints. Secondly, we decided to cut 4 same sides and connected them with 4 bars inner the diffuser like figure 4-25 and 4-26. However, to reduce the vortices and turbulence we must cut the inner bars as a following surface of the diffuser angle and we were unable to do that because it couldn't be cut by table saw. Therefore, we finally selected the present design that up and down sides would be bigger, and the bars were out of the sides as shown in figure 4-24.

Figure 4-24 Outer equipped Bar

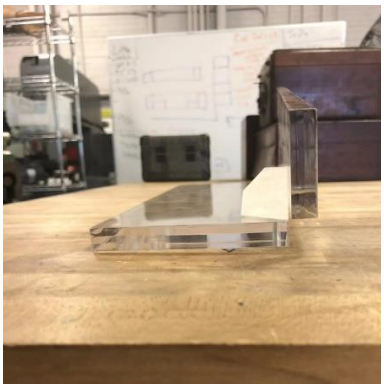

Figure 4-25 Inner Equipped Bar Test 1

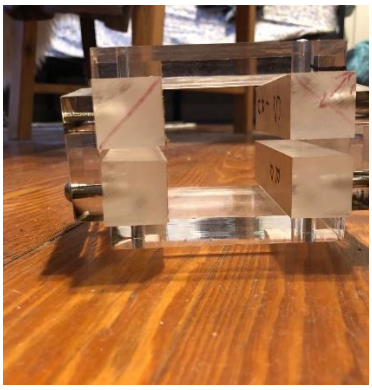

Figure 4-26 Inner Equipped Bar Test 2

4.1.5 Wide Angle Diffuser

Wide angle diffuser is made from acrylic sheets as well. It extended from 6 inch by 6 inch at inlet to 2 feet by 2 feet at outlet like settling chamber. As the length of the wide angle diffuser is 2 feet and its diffuser angle are 21 degrees, we chose 4 2 feet by 2 feet acrylic sheets to cut 4 trapezoid pieces and assembled them together with 4 0.5 inch by 0.5 inch acrylic bars. To made it easier to cut the sheet on table saw, we made a wooden tool to fix the acrylic sheet on so that we just required to push the wooden tool instead of pushing the angle of sheet, which is unstable. The wooden tool is shown in figure 4-31 and 4-32. It is also screwed by 0.25-inch-iong heat-set inserts. At inlet of wide angle diffuser where it would be connected to the corner, we added a flange shown in figure 4-33 and 3-D printed an adapter to transfer the structure from square to circle.

Figure 4-27 Wide Angle Diffuser 1

Figure 4-28 Wide Angle Diffuser 2

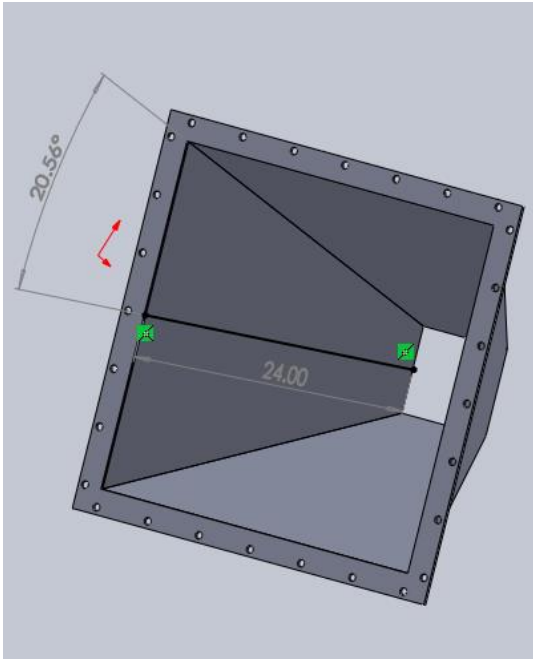

Figure 4-29 Design of Wide Angle Diffuser 1

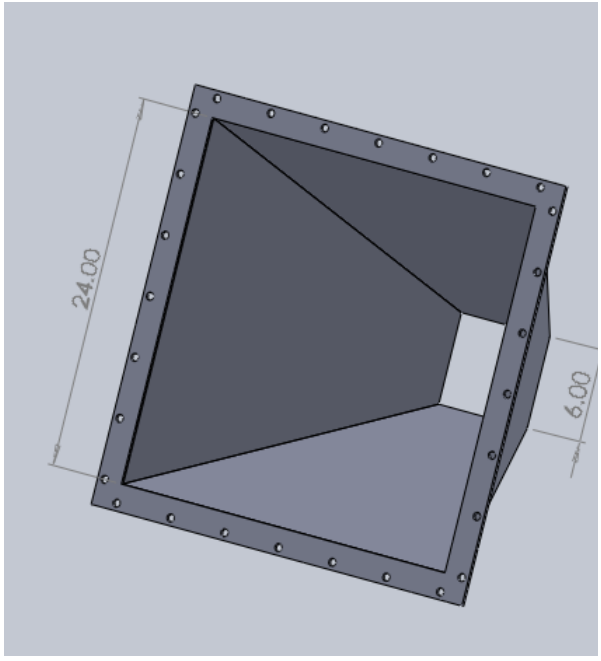

Figure 4-30 Design of Wide Angle Diffuser 2

Figure 4-31 Wooden Tools 1

Figure 4-32 Wooden Tools 2

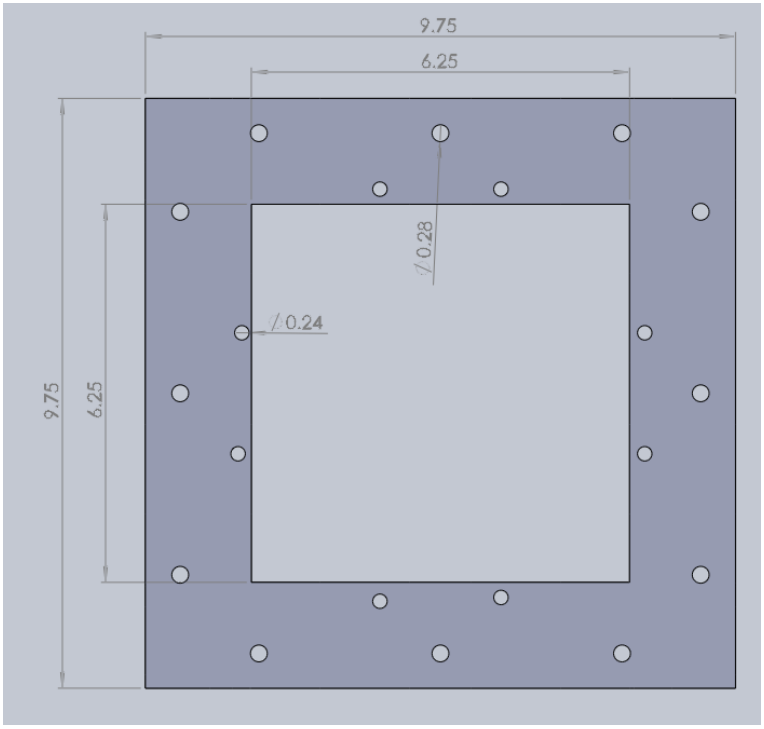

Figure 4-33 Flange of Wide Angle Diffuser Inlet

4.1.6 Assembly

After building each part of the wind tunnel, we required to assembly them together to get a whole Tufts Wind Tunnel. Firstly, we built a wooden frame to support the parts of diffuser, test section, contraction, settling chamber and wide angle diffuser, which is shown in the figure 4-1 above. To connect each part, we added flange to make it easier to screw them together, and all the flange size have been shown in the figure in the above parts. I used wing nuts to connect each part together because they are convenient to install and disassembly. In addition, I used some screw-mount nuts to hold the outlet of contraction and test section since their height was much smaller than other parts. These tools are shown in the following figures.

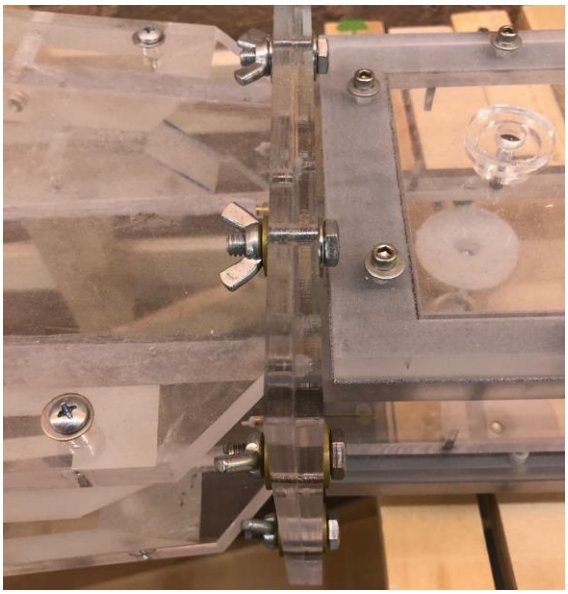

Figure 4-34 Usage of Wing Nuts

Figure 4-35 Usage of Screw-mount Nuts

4.2 *Experiments through Building*

Through our construction of wind tunnel, we use several experiments to help our building. This section will describe the Instron pull testing which is to check the pressure the diffuser structures can support.

Firstly, when we chose how to glue the two sides of acrylic pieces together, we designed three kinds of gluing ways: gluing on smooth surface, gluing on rough surface and gluing on finger joints. Figures of these three different gluing ways are shown below:

Figure 4-36 Gluing on Smooth Surface

Figure 4-37 Gluing on Rough Surface

Figure 4-38 Gluing on Finger Joints

We made these three testing pieces, which are all the size of 5 inch by 3 inch with their thickness of 0.5 inch, and then put them in the Instron device in Tufts Bray Lab like Figure 4-39.

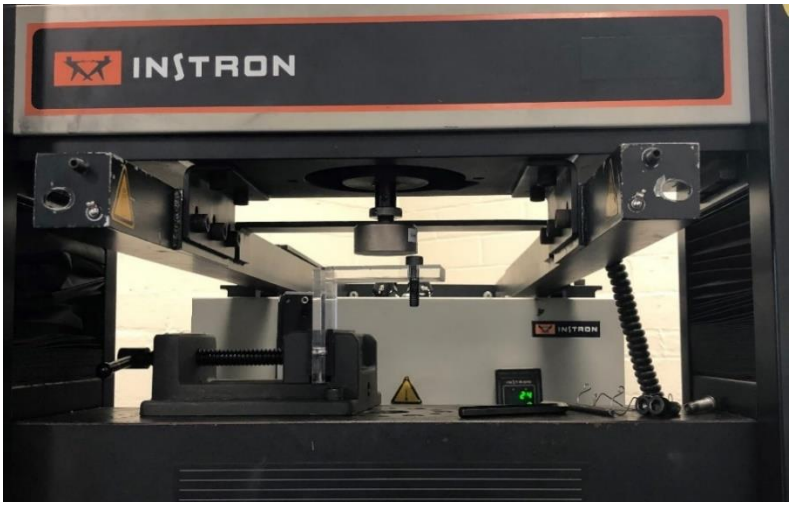

Figure 4-39 Testing Pieces in Instron

Table 4-1 Results of First Instron Test

The Method	Worst Load Applied (lb)	Safety Factor	Figure
Smooth Surface	22.5	2.1	4-36
Rough Surface	19.1	1.8	4-37
Finger Joints	57.3	5.5	4-38

Note: From last chapter we know the largest possible pressure would be 0.72 psi (for 0.5 Ma) so that the maximum applied load could be 0.72 psi*5 inches*3 inches = 10.5 lb. The maximum load:

$$F_{max} = \Delta pA \qquad (2)$$

While safety factor equals worst load applied on the test piece divided by F_{max}.

We put a screw in the hole of the piece to make a point where the loads can put on it and begin to add loads on the screw to see how many loads the piece could support before the joint place being destroyed. Finally, we found if we glued them on finger joints, it could hold on the most load which is 255 Newtons, while other two joints could only support fewer than 100 Newtons. However, the way of finger joints was not the possible way to build the whole diffuser and we selected another method to build (described in failures of diffuser design above).

Secondly, after we determined the way to build the diffuser, we also required a small testing piece to check if it could meet our pressure requirements. I built a 9-inch-long testing piece of diffuser while the real diffuser will be 47 inches long. It is shown as Figure 4-40 and 4-41.

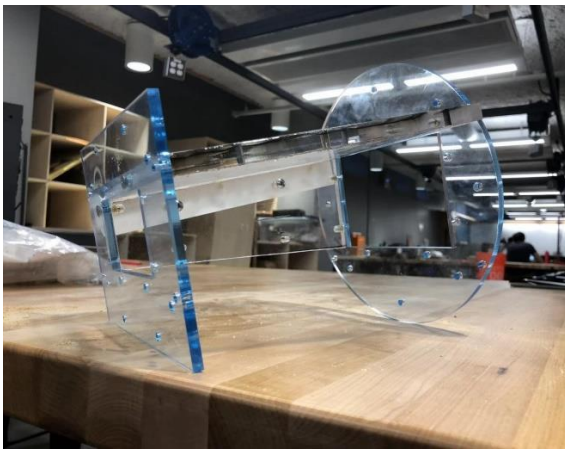

Figure 4-40 Testing Piece of Diffuser 1

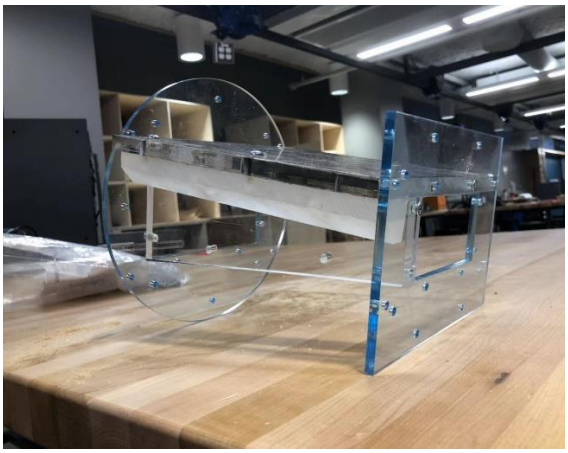

Figure 4-41 Test Piece of Diffuser 2

We put the piece in the Instron like figure 4-42 and 4-43 and found a support to hold the side because in real diffuser, there truly two sides to hold one side and we just required to make sure the place we glued would never be destroyed. As we added the most loads on these two sides and they never bent or came off, it should be the choice to build the whole diffuser.

Figure 4-42 Testing Piece of Diffuser of Side 1 in Instron

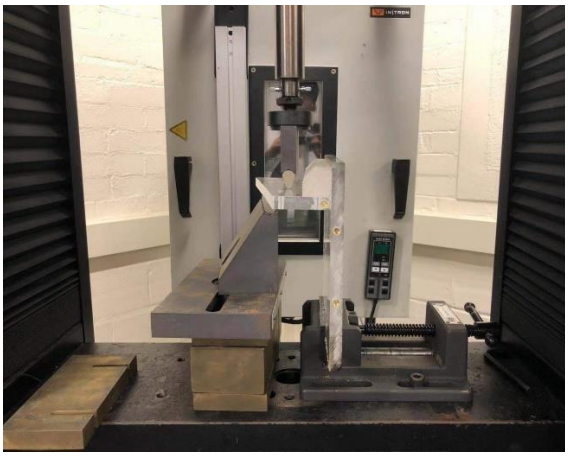

Figure 4-43 Testing Piece of Diffuser of Side 2 in Instron

Table 4-2 Results of Second Instron Test

Side	Load Applied (lb)	Safety Factor	Figure
Side 1	454	8.8	4-42
Side 2	236	10.4	4-43

Note: From last chapter we know the largest possible pressure would be 0.72 psi (for 0.5 Ma) so that the maximum applied load could be 0.72 psi*9 inches*8 inches = 51.84 lb (for the big side 1) and 0.72 psi*9 inches*3.5 inches = 22.68 lb. I didn't apply the worst load because I didn't want to destroy the test piece, but the safety factor was so big that it was very safe to build the real diffuser with this method.

5 Plans for Future Measurements

As we have built the almost whole wind tunnel, we want to use our Tufts Wind Tunnel to do some measurements and experiments. We can only make several plans for future measurements because of the lack of time. In this chapter, we will discuss the directions and details about the measurements we plan to finish.

5.1 *Static Pressure and Centerline Flow Speed*

In chapter 3 we have shown the flow speed and pressure drop in table 3-14, which is our calculation answers. However, we want to get the real value of our wind tunnel, so we require some equipment to measure the flow speed and static pressure. We select the pitot-static tube to measure the flow speed in the mean and the static pressure tap to measure the static pressure.

The pitot-static tubes are also called “Prandtl Tubes”, which is shown in figure 5-1. They are used as speedometers and can be put on aircrafts and in the wind tunnel to do several measurements, which is shown in figure 5-2 and 5-3. Normally, the pitot tube for testing the wind tunnel is around 2.5 inches long with a 0.125 inch diameter. There are some small holes drilled around the outside of the tube and a center hole down the axis of the tube. As the figure 5-1 showing, the small holes are connected to one side of the pressure transducer while the center hole is connected to another side separately. The pressure transducer is a device to measure the two different kinds of pressure: total pressure and static pressure by measuring the strain in a thin element an electronic strain gauge. To measure the flow speed, the center hole is pointed to the direction of the coming flow while the small holes are perpendicular to the centerline [21].

The function of the pitot-static tube is based on the Bernoulli's equation below:

$$P_{dynamic} = \frac{1}{2}\rho v^2 = P_{total} - P_{static} \quad (1)$$

Where ρ is the density of the flow and v is the flow velocity, which means we can gain the flow velocity of the flow by the following equation:

$$v = \sqrt{\frac{2(P_{total} - P_{static})}{\rho}} \quad (2)$$

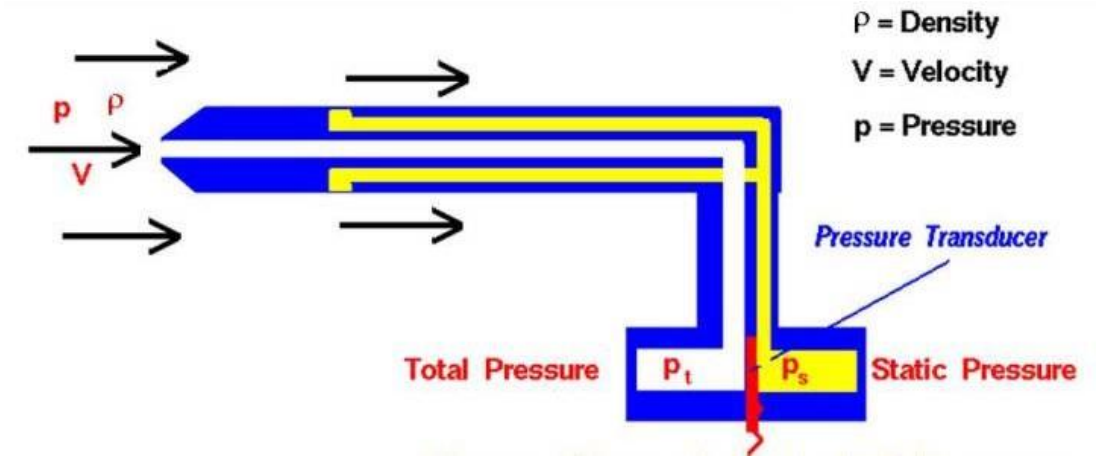

Figure 5-1 Pitot Static Tube
Take from NASA: https://www.grc.nasa.gov/www/k-12/airplane/pitot.html

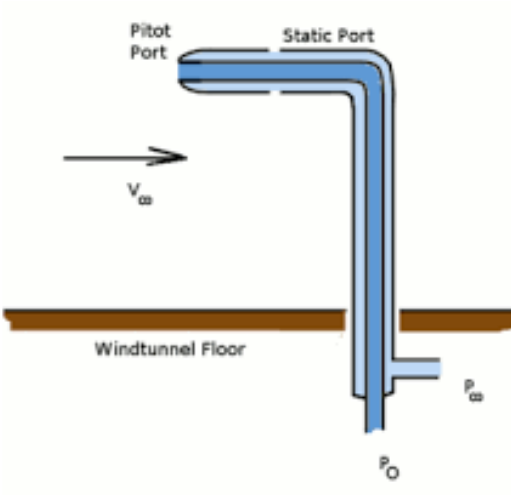

Figure 5-2 Pitot-static Tube in the Wind Tunnel taken from Aerodynamics for Students: http://www.aerodynamics4students.com/aircraft-instruments/

Figure 5-3 Pitot-static Tube on Aircraft taken from Student Pilot News: https://studentpilotnews.com/2019/07/22/quiz-pitot-static-system/

Static pressure taps are very small holes drilled perpendicular to the surface of the modal we want to measure where the flow streamlines are straight and connected to a pressure transducer located outside the wind tunnel model. Therefore, the pressure taps are usually applied with pitot-static tubes shown in figure 5-4. If the streamlines are curved, it is more useful to use a static pressure probe instead of a tap. In our wind tunnel, we can carefully use the tap to measure the static pressure in the test section while in contraction we can use static pressure probe. The tap's function is based on Bernoulli's equation as well [21].

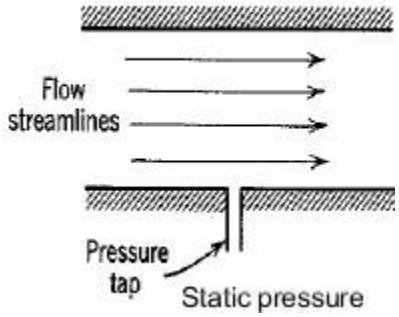

Figure 5-4 Wall Pressure Tap
taken from Slide Share:
https://www.slideshare.net/Apoorv00/ae547-3-pressuremeasurements

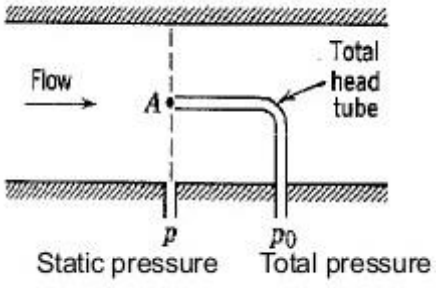

Figure 5-5 Simultaneous Measurement
taken from Slide Share:
https://www.slideshare.net/Apoorv00/ae547-3-pressuremeasurements

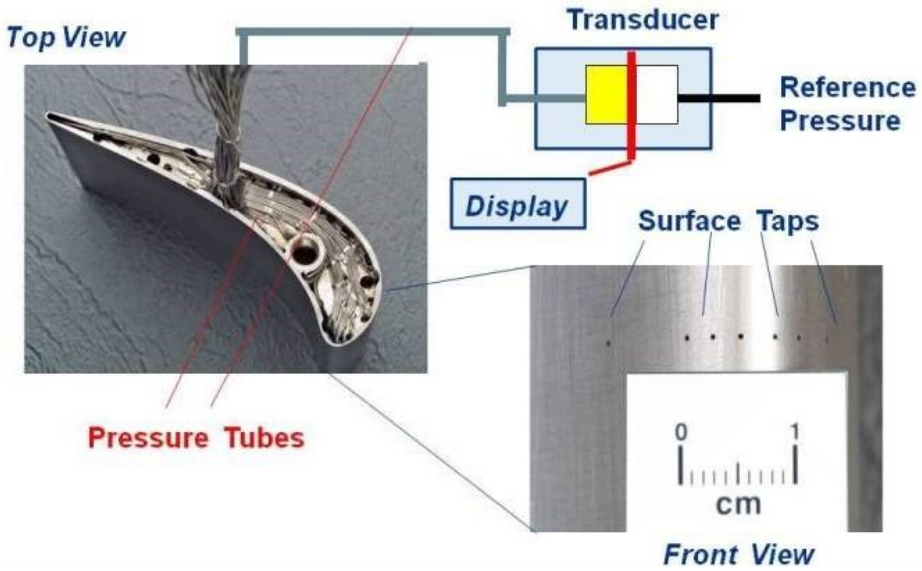

Figure 5-6 Static Pressure Measurement
taken from NASA: https://www.grc.nasa.gov/www/k-12/airplane/tunpsm.html

5.2 *Time Average Flow Field and Boundary Layer Profile*

The next level is to look at time average flow speed variation through the whole wind tunnel. We use the pitot-static tube to measure the time-averaged flow velocity as well. In the last section, we could gain pressure (based on Bernoulli's equation (1))from the pitot tube and use equation (2) to calculate the velocity of flow [22]. In this part, we focus on the spatial variation of flow speed instead of time fluctuations (turbulence), therefore, we could move the pitot-static tube through the test section and select two to three positions (across width or height, or several locations along the length) to do measurements to get the flow velocity variation vs. spatial position through the tunnel. Figure 5-7 shows the velocity profile changes with Mach number and position for the wind tunnel in Tohoku University, which is detailed in Chapter 2, and we want to get our Tufts Wind Tunnel velocity profile in a similar form.

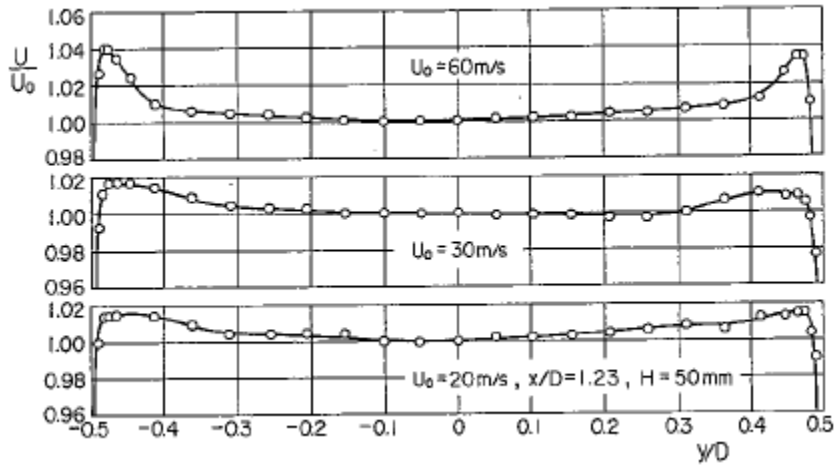

Figure 5-7 Velocity Profile vs. Mach Number and Position taken from Yasuaki Kohama's paper [23]

Where U_0 is the selected flow speed and we could calculate the Mach number by equation (1) in Chapter 2. x and y are the position through width and height. From above graph, we can see that velocity center point will seldom affected by Mach number and

position, it is very closed to flow speed we choose while on the boundary of the test section, the velocity will be increased at some degree. The faster of the flow speed, the more increasing be caused. To learn deeper about why the velocity is increased at the boundary, we must consider the boundary layer profile.

Boundary layer thickness is the distance across the boundary where the velocity reaches the free stream flow velocity U_0. Normally, it is defined as δ_{99} when

$$u(\delta_{99}) = 0.99U_0 \tag{3}$$

The equation to calculate the boundary layer thickness is different for laminar and turbulent flow. For a position x along the length:

$$\delta_{99L} = 5\sqrt{\frac{vx}{U_0}} = \frac{5x}{Re_x{}^{1/2}} \tag{4}$$

$$\delta_{99T} = \frac{0.37x}{Re_x{}^{1/5}} \tag{5}$$

Where ν is the kinematic viscosity and Re_x is the Reynolds number and

$$Re_x = \frac{U_0 x}{\nu} \tag{6}$$

The boundary layer profile could be shown as figure 5-8:

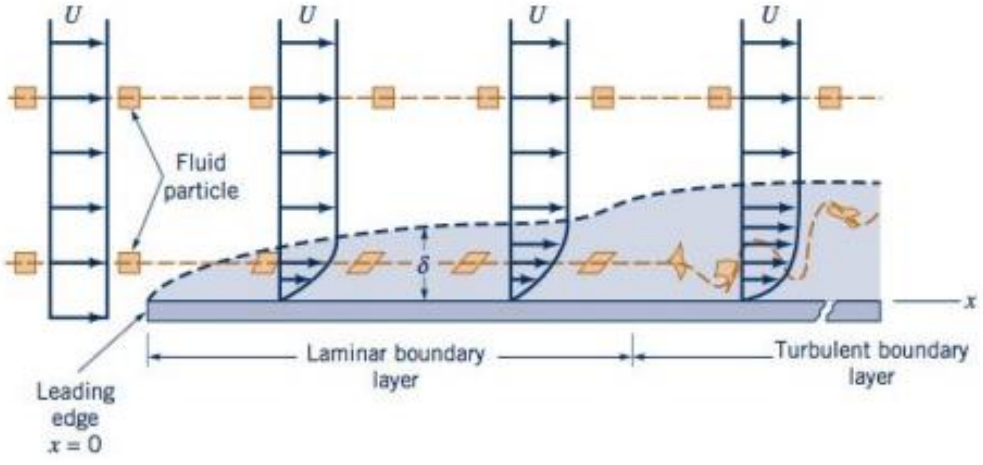

Figure 5-8 Boundary Layer Profile in one side of Test Section taken from Glover D C's paper [24]

we want to find the results of boundary layer thickness variation vs. position and Mach number. Like the figure 5-8, there should be three different curves for three different Mach number (to determine U_0). The bigger the Mach number is, the smaller the boundary layer thickness is, and the less time it takes to reach the free stream flow velocity.

5.3 *Turbulent Intensity*

To measure the turbulent intensity, we select the hot wire anemometers. Hot wire anemometers use the small electrically heated wire to measure flow velocity. When the flow goes across the heated wire, heat generated in the wire is dissipated to the surrounding environment because of the forced convection. There is a feedback control bridge to maintain the wire at a constant temperature by adjusting the current flow through the wire in response to the amount of heat loss [25-27,31]. The hot wire anemometer is shown in figure 5-9 and 5-10.

The principal based on the following equations. Since the loss of heat Q:

$$Q = I^2 R_{wire} = (A + BU^{\frac{1}{N}})(T_{wire} - T_{fluid}) \qquad (7)$$

Where A and B are constants depend on fluid properties and N is between 2 and 3. U is the mean flow velocity and T_{wire} and T_{fluid} are the temperature of wire and fluid. I is the electrical current passing through the wire and R_{wire} is the resistance of wire. If the temperature of flow is relatively constant, when the velocity increases, the heat loss from the wire increases. To cool the wire, the resistance of wire should be decreased by increasing the current flow through the wire [25-27].

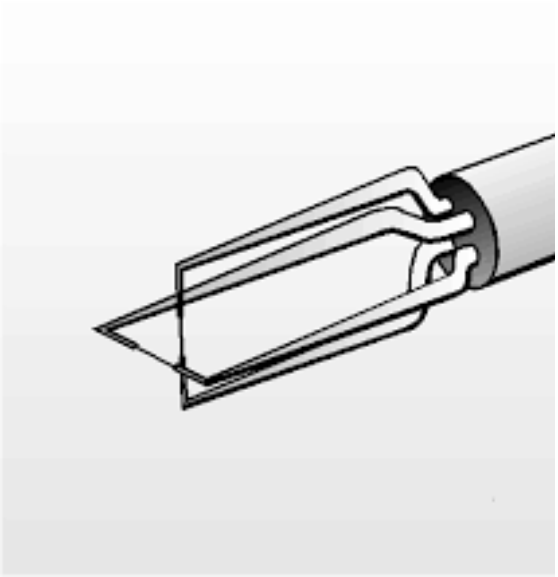

Figure 5-9 Hot Wire Anemometer Probe taken from F.E.Jorgensen's paper [25]

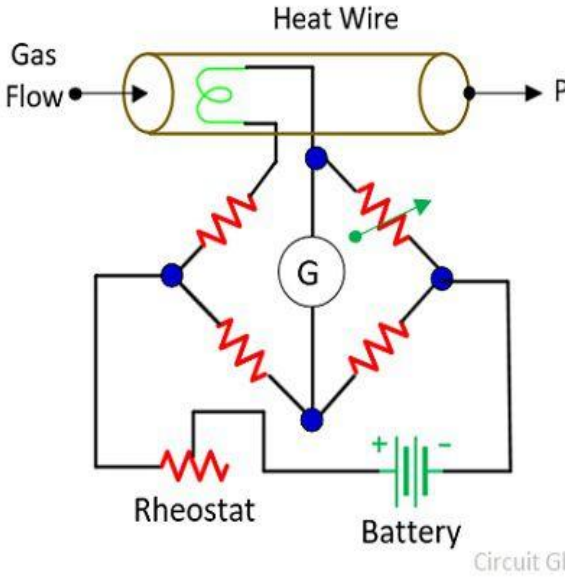

Figure 5-10 Hot Wire Anemometer Circuit taken from Circuit Globe: https://circuitglobe.com/hot-wire-anemometer.html

From the hot wire anemometer, we can obtain the mean flow velocity and the RMS value of the fluctuating velocity because the voltage across the bridge is directly proportional to the current through the wire. We can gain the output directly current voltage V_{DC} [26-28]:

$$V_{DC}{}^2 = V_0{}^2 + BU^{\frac{1}{N}} \tag{8}$$

Where V_0 is the voltage when flow velocity is zero. We also set:

$$u' = [\frac{1}{T}\int_0^T \left(\frac{du}{dt}\right)^2]^{\frac{1}{2}} \tag{9}$$

$$V_{RMS} = [\frac{1}{T}\int_0^T \left(\frac{dv}{dt}\right)^2]^{\frac{1}{2}} \tag{10}$$

And derived the equation (4) to get:

$$\frac{u'}{U} = V_{RMS}\frac{2NV_{DC}}{V_{DC}{}^2 - V_0{}^2} \tag{11}$$

And the mathematically definition of turbulent intensity %TI is from the equation below [26-28]:

$$\%TI = 100\frac{u'}{U} \tag{12}$$

Therefore, we calculate the turbulent intensity from the results we obtain from hot wire anemometer, which means it can be applied to measure the turbulence in the wind tunnel. We can put the hot wire anemometer in test section and keep the flow pass through to get what we want.

In chapter 2 we have given some examples of wind tunnel around the world and we have their turbulence intensity results as well. The low speed wind tunnel in University of Saskatchewan in Canada has the turbulence intensity at 0.6% through test section while the turbulence intensity of Glenn L. Martin wind tunnel in University of Maryland is 0.21% [17,19]. For the small low turbulence wind tunnel in Tohoku University in Japan, there are two pictures to show the experiments results of the turbulence measurements.

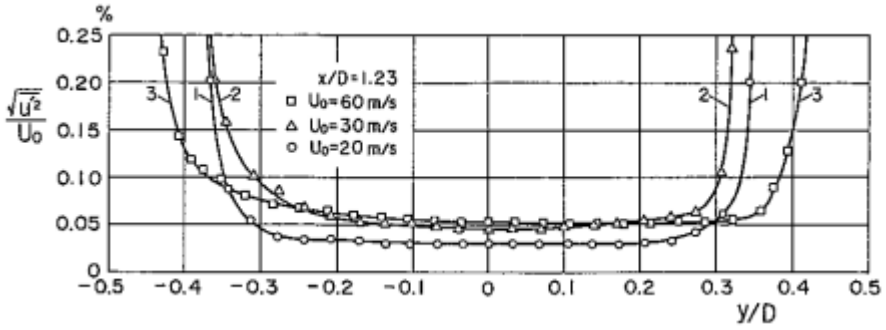

Figure 5-11 Turbulence Intensity in Test Section in Horizontal Direction vs. Different Velocity taken from Yasuaki Kohama's paper [23]

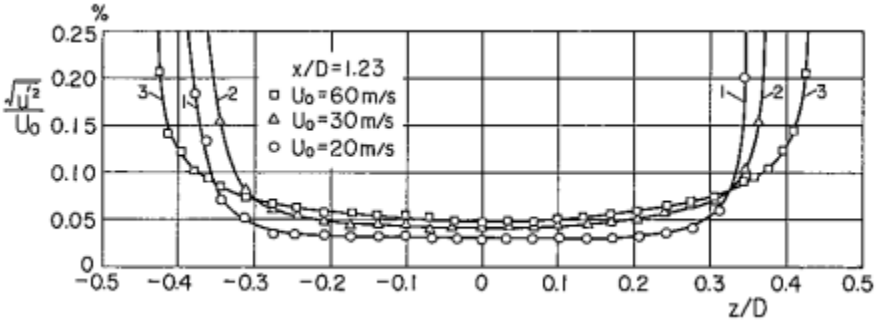

Figure 5-12 Turbulence Intensity in Test Section in Vertical Direction vs. Different Velocity Taken from Yasuaki Kohoma's paper [23]

Where U_0 is the flow velocity and D is the size of test section in each direction. From these two graphs, we can see the turbulence intensity is about 0.25% [3]. For our Tufts Wind Tunnel, we might set a range of 0.2% to 0.5% as a suitable turbulence intensity level.

5.4 *Microphone Array and MEMS Sensor Wall Mounting*

In the past Prof. White and his students did several examples to mount the microphone array and MEMS sensors. We can gain some experience from these examples and find suitable methods to mount these two things on our Tufts Wind Tunnel. The microphone array was flush mounted into a precision machined square cutout in an aluminum plate, and sides were sealed with modeling clay and smoothed flat with a razor blade. After doing these we put the plate into the side of the test section whose size is 15 cm by 15 cm, so that the microphone array was mounted on the surface of the duct to do tests as shown in figure 5-13 [12].

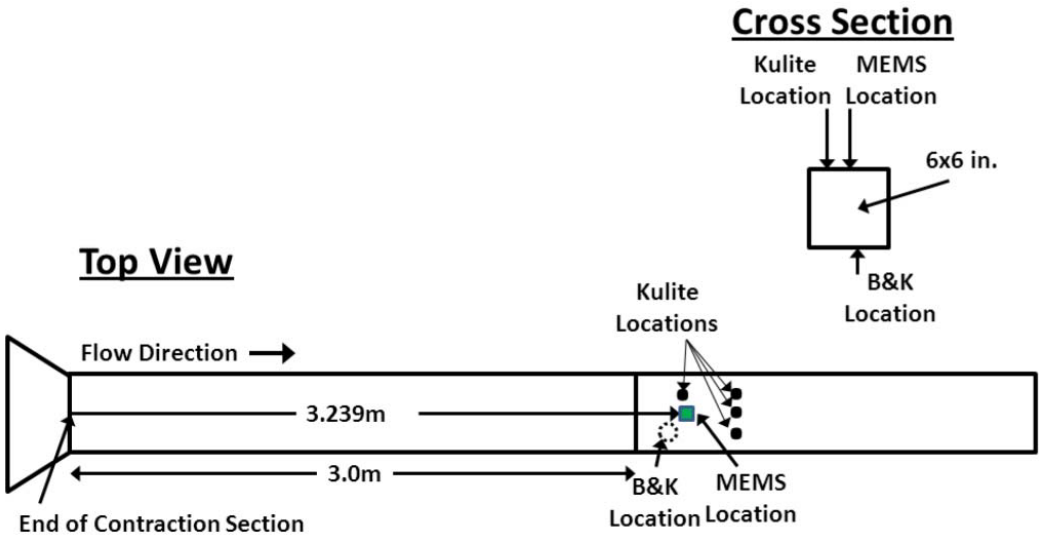

Figure 5-13 Microphone array mounting taken from Krause J S's paper [11]

For the MEMS sensor, we flush mounted it in a nickel painted acrylic plate in the floor of the test section, locating at 65 cm away from the outlet of the contraction. Figure 5-14 shows how we mounted the MEMS sensor in the test section to measure the shear stress [14].

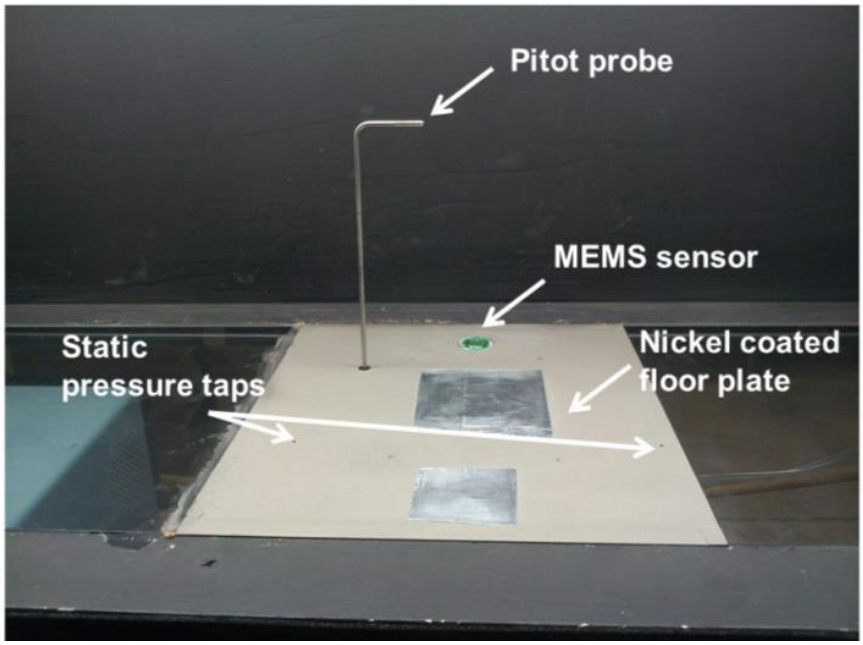

Figure 5-14 Mounting the MEMS Sensor in Test Section Surface
taken from Zhengxin Zhao's paper [14]

Since our test section is smaller and the passing flow is faster, we must find our own methods to mount the microphone array and MEMS sensors. We can add an aluminum plate upon the down wall of the test section with sensors mounted on it. However, instead of replacing part of the side, we can just glue the plate on the side keeping its surface smooth (there is a small gap between the flange and the main part of test section, maybe we can prevent it by this way).

Except mounting the microphone array and MEMS sensors, we can do also experiments as well. One is to modify the wall situation to modify the shear. We could put these kinds of experiments together with the measurements of pressure and velocity

with pitot-static tube and pressure tap. It is easier to replace part of the wall by some medal plates which is easy to mount elements on them because it requires more space to put so many items in our small test section. To modify the wall situation (wall roughness), we have several plans: just flat plate, small hexagonal mesh elements, glass beads, several cubic blocks ranging by rows like figure 5-15. Instead of only doing on the flat plate, we can use curved surface by substitution to create pressure gradient in one or two dimensions (on one or two or more walls), and add a backward or forward facing step or hence to create a stagnation region. We want to see the flow profile in different flow structure in test section.

Figure 5-15 Wall Modification in Tunnels
taken from Zhengxin Zhao's paper [14]

6 Conclusions and Future Work

In this chapter, I will highlight in more details about works done in this work and also in future works that can be planed and used to improve our present works.

6.1 Conclusions

The goals in the design of a wind tunnel is to make it a low cost, high efficiency and suitable size for our lab wind tunnel with methods to reduce the turbulence in test section. In chapter 2, we looked at several different universities' wind tunnels as examples and find many interesting tunnels. Some of them are small size by with a high speed while some are much bigger but their flow is slower. They are mostly subsonic or supersonic wind tunnels and we focus on their structure and size to figure out which part should we select on our own wind tunnel and what size will we design. We designed the size of test section at 2" by 4" and the flow velocity moving pass it is 0.5 Mach. The microphone arrays and MEMS sensors which are built and tested by past Tufts work are also mentioned because we want to use these two things to measure how our wind tunnel works.

To determine the choice of blower and materials and structures of each part through wind tunnel, we calculated the pressure drop in each part: test section, contraction, settling chamber, diffuser, wide angle diffuser, return duct and corners which shown in chapter 3. The total pressure drop through the wind tunnel is almost 5000 Pa while the pressure drop in test section is nearly 1000 Pa. The pressure drop in diffuser becomes the biggest part and it is over 2500 Pa. In addition, we gain the flow velocity in each part as well which can help us select the size of each part and make sure the flow can really move through the tunnel.

Chapter 4 shows details of how we built the follow part: test section, contraction, settling chamber, diffuser and wide angle diffuser. The flow in the wind tunnel comes from the blower, and after moving pass the return duct and three corners, it reaches wide angle diffuser, then settling chamber, contraction, test section and diffuser, and finally reaches blower to finish a closed circulation. All the walls of each part were made from 0.5”-thick acrylic sheets (except contraction).

For test section, we used acrylic as materials because its surface is smooth enough and its structure can support the atmosphere pressure. There are four walls of test section and the up and down sides can be unfixed which is easy to modify the part. Between each part, there are flanges to connect and fix all these parts, and we used wing nuts to fix the screws. All the flanges are cut from ¼”-thick acrylic sheets by laser cutting.

For contraction, it is the only one that wasn’t made by acrylic but we chose fiber glass because it is a curved-surface part and it is easier to use fiber glass than to cut acrylic pieces. The inlet size of contraction is 2’ by 2’ and its outlet size is the same as test section.

For settling chamber, we made it by acrylic as well and it looks like an apparent square box without up and down covers. The flange of settling chamber are divided into several pieces because the size of settling chamber is so big (the same as inlet size of contraction) that we could not cut a whole flange in laser cutting.

For diffuser, it is the longest part among parts we built as it is almost 4 feet long. We divided it into two parts to make it easier to cut in laser cutting and added joints to connect and fix these two part as a whole thing. The inlet size of diffuser is the same as test section while the outlet size is based on the size of blower, and we designed it as a square (the length of four sides of diffuser is the same). It took most time to build because we chose

many plans to design its four walls and how to connect these four walls. At last we selected the outer-fixed acrylic bars to connect all the sides, which is stable when holding on the atmosphere pressure. We specially did tests on Instron device to make sure our structure is safe.

For wide angle diffuser, its outlet size is the same as settling chamber and its inlet size is based on the size of corners. We used table saw to cut all four walls of wide angle diffuser. To make it easy to cut, we also built a wooden support to fix the sheets when cutting instead of holding the angle to the edge of table saw when moving, which is unstable and unsafe.

Finally, I built a wooden frame to support the part we have already made and used screw-mount nuts to hold each part where they do not directly touch the wooden frame.

6.2 Future Work

After we build the whole Tufts Wind Tunnel, I think we have several future works to do. Firstly, there should be more works on the Tufts Wind Tunnel itself. Since we have already built the test section, contraction, settling chamber, diffuser and wide angle diffuser, we should buy the corners, the return duct and the blower and assembly all the part together to become a whole wind tunnel. We should also check each part to see if there are any leaks or other gaps and destructions that may affect the flow, we can use RTV to prevent leak.

Secondly, there are several plans for future measurements. We can use pitot-static tube to measure the static pressure and centerline flow speed, and use static pressure tap to measure straight streamline pressure. We can use hot wire anemometers to measure the turbulent intensity as well. In addition, looking at time averaged flow velocity variation

through space and the boundary layer profile. We want to find how the location of flow affect the flow speed. What's more, we can find methods to mount the microphone array and MEMS sensors on the wall of test section or other part of the tunnel, and other experiments we can do with modification of the wall situation like change the roughness of the wall.

References

[1] Libii, Josué Njock. "Wind Tunnels in Engineering Education." *Wind Tunnels and Experimental Fluid Dynamics Research* (2011): 235-260.

[2] Calautit, John Kaiser, et al. "A validated design methodology for a closed-loop subsonic wind tunnel." *Journal of Wind Engineering and Industrial Aerodynamics* 125 (2014): 180-194.

[3] Mehta, Ravi Datt, and Peter Bradshaw. "Design rules for small low speed wind tunnels." *The Aeronautical Journal* 83.827 (1979): 443-453.

[4] Cattafesta, Louis, Chris Bahr, and Jose Mathew. "Fundamentals of wind-tunnel design." *Encyclopedia of Aerospace Engineering* (2010).

[5] Eckert, William T., Kenneth W. Mort, and Jean Jope. "Aerodynamic design guidelines and computer program for estimation of subsonic wind tunnel performance." NASA Technical Note, NASA TN D-8243, October 1976.

[6] Peñaranda, Frank E., and M. Shannon Freda. "Aeronautical Facilities Catalogue. Volume 1: Wind Tunnels." NASA RP-1132, 1985.

[7] Vlajinac, Milan. "Design, Construction and Evaluation of a Subsonic Wind Tunnel." Diss. Massachusetts Institute of Technology, 1970.

[8] Ronglin Wu, Yuzhen Wang. "Design Principles of Wind Tunnel." *Beijing Aviation Academy Press,* 1985.

[9] Welsh, Andrew, "Low Turbulence Wind Tunnel Design and Wind Turbine Wake Characterization". *Theses and Dissertations*. 180. (2010).

[10] Bradshaw, Peter, and R. C. Pankhurst. "The design of low-speed wind tunnels." *Progress in Aerospace Sciences* 5 (1964): 1-69.

[11] Kulkarni, Vinayak, Niranjan Sahoo, and Sandip D. Chavan. "Simulation of honeycomb–screen combinations for turbulence management in a subsonic wind tunnel." *Journal of wind engineering and industrial aerodynamics* 99.1 (2011): 37-45.

[12] Krause, Joshua S., et al. "A microphone array on a chip for high spatial resolution measurements of turbulence." *Journal of microelectromechanical systems* 23.5 (2014): 1164-1181.

[13] Zhao, Zhengxin, et al. "A microfabricated shear sensor array on a chip with pressure gradient calibration." *Sensors and Actuators A: Physical* 205 (2014): 133-142.

[14] Zhao, Zhengxin, et al. "Flow testing of a MEMS floating element shear stress sensor." *52nd Aerospace Sciences Meeting*. 2014.

[15] "Small low-turbulence wind tunnel," Institute of Fluid Science, Tohoku University, 2010. [Online]. Available: http://homepage.usask.ca/~drs694/research%20facilities.htm. [Accessed 4 July 2011]

[16] "Wind Tunnel Courses," School of Aeronautics & Astronautics, Purdue University, 2018 [Online]. Available: https://engineering.purdue.edu/AAECourses/Raisbeck/wind_tunnels.htm.

[17] David Sumner. "Research Facilities and Instrumentation," Department of Mechanical Engineering, University of Saskatchewan, 2019 [Online]. Available: http://homepage.usask.ca/~drs694/research%20facilities.htm. [Accessed 10 February 2019]

[18] “Wind Tunnels,” College of Engineering: Aerospace Engineering, University of Michigan [Online]. Available: https://aero.engin.umich.edu/research/facilities/wind-tunnels/. [Accessed 15 May 2012]
[19] “Glenn L. Martin Wind Tunnel,” A. James Clark School of Engineering, University of Maryland, 2020 [Online]. Available: https://windtunnel.umd.edu/facilities.
[20] “Facilities in High-speed Aerodynamics and Propulsion Laboratory,” A. James Clark School of Engineering, University of Maryland, 2018 [Online]. Available: http://www.hyper.umd.edu/facilities/index.html, [Accessed summer 2017]
[21] Beck, B. Terry. "AC 2010-1803: the aerodynamics of the pitot-static tube and its current role in non-ideal engineering applications." American Society of Engineering Education Annual Conference, June 2010, Louisville, Kentucky.
[22] Ristić, Slavica, et al. "Review of methods for flow velocity measurement in wind tunnels." *Sci. Rev.* 54.3 (2004).
[23] Yasuaki Kohama. “Measurement Report of Performance of a Low Turbulence Wind Tunnel.” *The Memoirs of the Institute of High Speed Mechanics*, Tohoku University. Vol. 48 (1982). 119-422
[24] Glover, Daniel C., Liam M. Madden, and Robert J. Cabri. "Leading Edge Boundary Layer Suction Device for the Cal Poly Rolling Road Wind Tunnel." Department of Mechanical Engineering, California Polytechnic State University, San Luis Obispo (2017).
[25] F.E.Jorgensen. “How to Measure Turbulence with Hot-wire Anemometer – A Practical Guide,” 2002 [Online]. Available: http://web.iitd.ac.in/~pmvs/courses/mel705/hotwire2.pdf, [Accessed 1 February 2002]
[26] Miller, William R. “Hot wire anemometer investigation of turbulence levels and development of crystal flow visualization techniques for the rectilinear cascade test facility”. Diss. Monterey, California. Naval Postgraduate School, 1979.
[27] Cooper, Ralph D., and Marshall P. Tulin. “Turbulence measurements with the hot-wire anemometer”. North Atlantic Treaty Organization, Advisory Group for Aeronautical Research and Development, 1955.
[28] Knudsen, James G., Donald L. Katz, and Robert E. Street. "Fluid dynamics and heat transfer." *Physics Today* 12 (1959): 40.
[29] Almeida, Odenir de, et al. "Low Subsonic Wind Tunnel-Design and Construction." *Journal of Aerospace Technology and Management* 10 (2018).
[30] Arifuzzaman, Md, and Mohammad Mashud. "Design construction and performance test of a low cost subsonic wind tunnel." *IOSR Journal of Engineering* 2.10 (2012): 83-92.
[31] Farell, C., and Youssef, S. (March 1, 1996). "Experiments on Turbulence Management Using Screens and Honeycombs." ASME. *J. Fluids Eng.* March 1996; 118(1): 26–32.
[32] Ghorbanian, Kaveh, Mohammad Reza Soltani, and Mojtaba Dehghan Manshadi. "Experimental investigation on turbulence intensity reduction in subsonic wind tunnels." *Aerospace science and Technology* 15.2 (2011): 137-147.
[33] Santos, Alessandra Maciel dos, et al. "Effects of screens set characteristics on the flow field in a wind tunnel." *Journal of Physics: Conference Series*. Vol. 733. No. 1. IOP Publishing, 2016.